# A study of the feasibility of molybdenum$^{99}$ production by neutron capture of molybdenum$^{98}$ in a mini loop using natural convection

Rona Roovers

Student number: 4690494

# Abstract

Technetium[99], the most used medical isotope, is obtained by the decay of molybdenum[99]. Molybdenum[99] can be created in several ways. In this thesis, the method of neutron capture by molybdenum[98] is looked into.

As setup a cylindrical tube in the form of a parallelogram next to the HOR reactor is used, HEAL (HOR Experimental Activation Loop). Inside this cylindrical tube a solution of molybdenum[98] is present. The walls of the tube are heated by gamma heating. By varying the thickness of the wall, natural convection causes the fluid to flow inside the tube.

Dresen [18] and Haffmans [19] already looked into a system for the creation of molybdenum[99] with a setup of the same shape and an active pump for cooling. They made use of the fission of uranium[235]. Dresen used a time independent, steady state method and Haffmans made use of a time dependent method, both numerical. A pump could malfunction, which can cause problems in this system, so in this thesis a setup without a pump as cooling system is investigated.

In this thesis, three methods were used to calculate the temperature profile and velocity in the system. Firstly, a time dependent numerical method was used, which made use of the Runga Kutta method. Secondly, a time independent numerical method in which the Newton Raphson method was used. Lastly, an analytical method was derived.

The time dependent numerical method was used to determine if the system will go towards a steady state. The time independent numerical method and analytical method were both made to obtain results more quickly for later analyses. Which of these two methods was used was dependent on the correctness of the results. The time dependent numerical method showed that this system will go towards a steady state, which was used for the initial conditions for the time independent methods. The steady state solutions for the time dependent and the time independent numerical methods were effectively the same. The solution of the analytical method was of the same shape but slightly shifted in value. This is probably caused by simplifications in the analytical method. The system seems to have a stable steady state solution. The values of these solutions are very dependent on the thickness of the wall and the radius of the tube.

However, the molybdenum[99] production that this system can achieve is relatively low, with an order of magnitude of around $10^{-8}$ milligram molybdenum[99] per week. This is due to the fact that molybdenum[98] has a small neutron cross section.

# Contents

# 1  Introduction

Medical isotopes are often used in hospitals. The most common isotope used for diagnosis is technetium[99] [1]. This isotope is ideal for medical diagnosis. This is because the six hours half-life makes it usable for diagnostics, the emitted gamma rays can be well detected and the patient will experience low doses of radiation [2]. This medical isotope is almost always produced by the decay of molybdenum[99], this has a half-life of around 66 hours. The 66 hours half-life of molybdenum[99] is useful for the delivery of the isotope to the hospitals.

So the creation of molybdenum[99] is quite crucial. At the moment the biggest producers of this isotope can be found in the Netherlands, Belgium, South Africa, Poland and Australia [1]. Different methods to create molybdenum[99] are visible in figure 1.
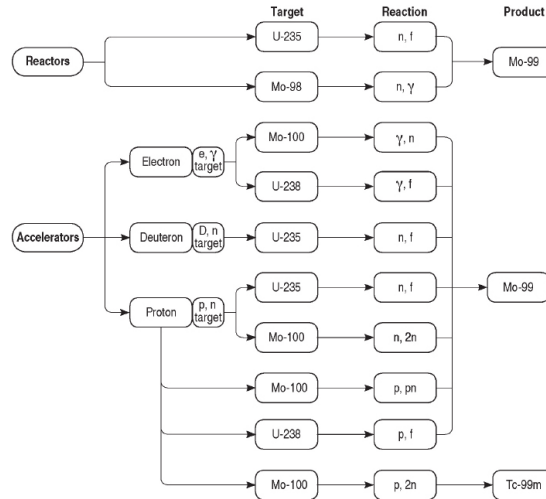


Figure 1: *Different methods to obtain molybdenum[99] [2].*

This thesis will focus on the production of molybdenum[99] in a reactor, for this two methods can be used, as can be seen in figure 1. The method using uranium[235] has been researched in several previous papers. A relatively large system loop was researched, by Huisman [21], by Elgin [20], by Huisman [22], by Pothoven [23] and by Pendse [24]. This included research with a pump to create a flow inside the loop and without a pump. In the later case, the flow inside the loop was induced by natural convection. This system had promising results. However, for safety reasons the used volume is too large. So a smaller system is needed. Haffmans [19] and Dresen [18] already looked into a smaller setup next to the reactor core in the Hoger Onderwijs Reactor, the HOR. This setup uses a cooling system with a pump and natural convection.

This thesis will look into the feasibility of a setup with only natural convection, so without a pump. This is done because a pump could cause difficulties when it malfunctions. Also, a different production method is used. Namely production via neutron capture by molybdenum[99], as seen the second method in figure 1. This method gives less isotopes which have to be stored as waste than the fission method used in previous researches.

The setup used in this thesis, HEAL (HOR Experimental Activation Loop), is of similar shape as the setup used by Haffmans [19] and Dresen [18]. It consists of a circular pipe in the form of a parallelogram, as seen in figure 2.



(a) *A side view of the setup used in this thesis. The red region is the region inside the tube where the fluid is heated and the dark blue region is the region inside the tube were the fluid is cooled.*

(b) *A top view of the setup used in this thesis. With the reactor core visible next to the DLDR tube.*
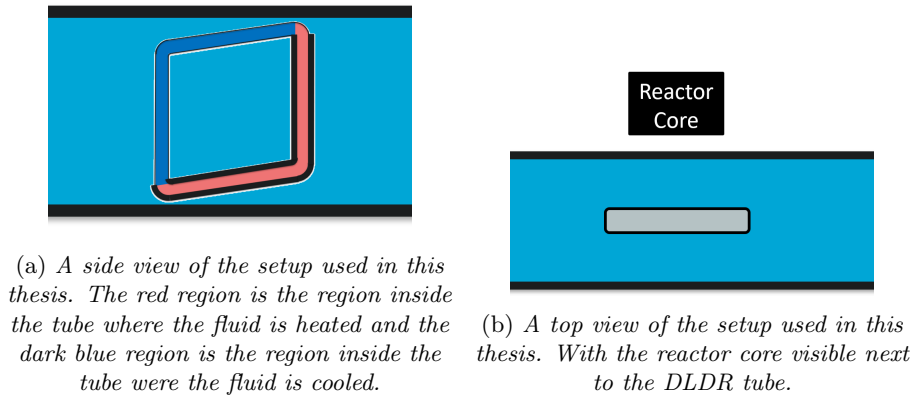
Figure 2: *A view of the setup, the blue region is the water surrounding the setup inside the DLDR tube*

In figure 2b the gray part in the middle represents the fluid inside the tube and the black edges which enclose the gray area is the wall of the HEAL tube. The black edges which enclose the dark blue and red area in figure 2a also represents the wall of the HEAL tube. It can also be seen that the setup will be placed inside a bigger tube, this is the DLDR tube in the HOR, which is located next to the reactor [19]. The walls are varied in thicknesses as seen in figure 2a, this is done to accomplish natural convection. This will occur since there will be heat generation inside the walls of the tube. The heat generation is dependent on the volume of the wall, following from the thickness of the wall. The lower horizontal and the right vertical parts of the tube will be thicker, which causes heating of the fluid. The upper horizontal part and the left vertical part will have a thinner wall, which causes less heating inside the wall and more heat transfer to the surrounding water. Resulting in the cooling of the fluid in these regions. This will be further elaborated in section 2.

Thus, this thesis will make use of neutron capture by molybdenum$^{98}$ for the production of molybdenum$^{99}$. The gamma heating in the wall of the tube in the setup causes natural convection.

## 1.1 Goal and outline

This thesis will approach this system in the following three different ways:

- Time dependent numerical method, using the Runga Kutta method.

- Time independent numerical method, using Newton Raphson method.

- Time independent Analytical method.

These last two are assuming the system to be in steady state, the first method will check if the system will indeed reach a steady state.
The goal of this thesis is to answer the following three questions:

– What influence do the measures of the setup have on the natural convection within this system?

– What will the production be which can be achieved by this system?

– Are the numerical and analytical results in agreement?

  ⋄ If there are any differences, what is the cause of these differences?

An answer to the first question is desired because the temperature of the fluid should stay below $90^o$C for safety, because boiling fluid inside this system could be dangerous. This question will be answered by varying the measures in the setup geometry.

An answer to the second question determines if this setup is suitable as a replacement for the current setup for molybdenum$^{99}$ production. This answer will be obtained by calculating the production.

Finally, an answer to the last question will determine if the used methods are consistent, the methods are usable and which of these methods is most suitable to use for this system. For this, the result of the numerical and analytical method will be compared.

First, the design of the used setup will be clarified in section 2, then in section 3 the theory applicable to this system will be stated. Next in section 4 the derivations needed in this thesis will be stated and the methods will be described. The results obtained in this thesis will be shown and discussed in section 5. Section 6 contains the conclusion of this thesis and recommendations for following researches on this topic.

# 2 Design

## 2.1 The loop

In this thesis a similar shape will be used for this system as used by Dresen [18] and by Haffmans [19]. This shape can be seen in figure 3a. Unlike Dresen [18] and Haffmans [19] no active cooling system is used. Instead, there will be different thicknesses, $\delta R$, of the walls. This gives a different intersection at different locations in the tube, such an intersection is visualized in figure (3b). Due to the slight angle, $\phi$, the direction of the velocity of the fluid is set. In this case, the flow will be counterclockwise, if the angle becomes negative, the flow will be clockwise.

The setup will be placed in the DLDR tube in the Hoger Onderwijs Reactor, HOR, of the TU Delft, which is located close to the reactor core. The DLDR tube is filled with water. The average temperature of the water inside this tube is $40^oC$.



(a) *Shape of system side view.*

(b) *Intersection of tube.*
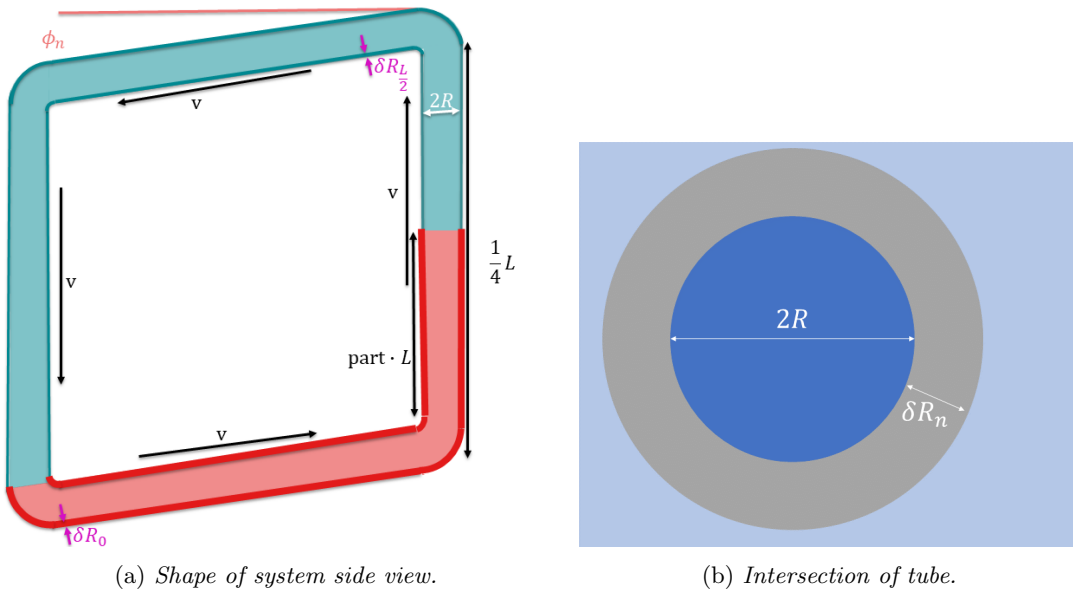
Figure 3: *Design of the system, $\delta R$ is the thickness of the wall, $R$ is the radius of the inner tube, $v$ is the velocity of the fluid inside the tube, $\phi$ is the angle the horizontal pipe has with the x-axis, $L$ is the total length of the tube and part is the part of the length in which the lower tube will have a thicker wall.*

### 2.1.1 Length of the loop

In this thesis, the four different parts of the tube will have the same length. Since this setup will have to be placed in the DLDR tube, there will be a constraint on the length of the tube. The diameter of the DLDR tube is $D_{\text{DLDR}} = 0.140$ m. So the diameter of the DLDR tube has to be bigger than the summation of the following parameters: The length of one quarter of the tube; The thickness of the wall in the upper tube; The thickness of the wall in the lower tube; The diameter of the inner tube and the length in the vertical direction of the nearly horizontal tubes caused by the angle. This correlation is described in equation (2.1),

$$D_{\text{DLDR}} > \frac{L}{4} + \delta R_0 + \delta R_{\frac{L}{2}} + 2R + \frac{L}{4}\sin(\phi). \tag{2.1}$$

In equation (2.1) the following parameters are used, the total length of the tube given by $L$, the radius of the inner tube given by $R$, the angle of the nearly horizontal tubes given by $\phi$ and the thickness of the wall of the tube at the lower horizontal tube and at the upper horizontal tube

given by $\delta R_0$ and $\delta R_{\frac{L}{2}}$ respectively.

When this is rewritten as a constraint of the total length of the tube, equation (2.2) is obtained,

$$L < \frac{4(D_{\text{DLDR}} - \delta R_0 - \delta R_{\frac{L}{4}} - 2R)}{1 + \sin(\phi)}. \tag{2.2}$$

So for this system, equation (2.2) will be used as a constraint for the length of the tube.

### 2.1.2 Thickness of the wall

As stated earlier there will be different thicknesses of the wall in the tube. This has been depicted in figure 3a. In this figure, it can be seen that the lower horizontal part will have a thicker wall than the upper horizontal part and the left vertical part. The lower part of the right vertical part also has a thicker wall, while the upper part of the right vertical part will have a thinner wall. The length, 'part · L', of this lower part will later in this thesis be varied.

The different thicknesses of the wall result in a moving fluid inside the tube, because heat generation occurs inside the wall due to gamma radiation. This heat generation is dependent on the thickness of the wall. The wall can both heat the fluid inside the tube and the surrounding water outside the tube. The effect of this heat generation and the design of the loop is that the fluid inside the tube will be heated in the lower horizontal tube and partly in the right vertical tube. The upper horizontal tube and the left vertical tube have thinner walls, this results in less heat generation inside these parts. If the wall is thin enough the temperature of the wall can be lower than the temperature of the fluid inside the tube. This is because the wall is cooled by the water surrounding the tube. When this is the case energy will be transported from the fluid inside the tube to the wall and after that to the surrounding water. In other words, the fluid inside the tube will be cooled. This causes the fluid to be moving inside the tube, since the heated fluid will get a lower density causing this fluid to move upwards, this fluid will be cooled in the upper part causing the density to drop again, which makes the fluid going downwards.

The thickness of different tubes will be adjusted to investigate the effect of the thickness of the wall on the velocity in the system and on the temperature profile.

### 2.1.3 Quantity of the fluid

The quantity of the fluid inside the tube will determine the production of molybdenum[99]. Since there is a higher production for a larger quantity of fluid, the volume of this fluid has to be as large as possible. For the length of the tube, there is already a constraint. So it is preferable to have the radius of the inner tube as large as possible. For a larger inner tube, a thicker wall is needed to heat the fluid, to create natural convection. So at which radius of the inner tube there is still a working system will be investigated.

To determine the production, the volume of the fluid is needed. This volume is described in equation (2.3),

$$V_{\text{fluid}} = \pi L R^2. \tag{2.3}$$

## 2.2 Materials

The materials used in this system are discussed in this subsection. The system used will have three different materials: one for the wall, one for the fluid inside the tube and water for the surrounding environment.

### 2.2.1 Material of the wall

A zirconium alloy is used by previous researches with an almost similar loop, see Dresen [18] and Haffmans [19]. This material has good corrosion resistance and a low thermal neutron cross section. So this material is for this system also a proper choice.

### 2.2.2  Material of the fluid

The material for the fluid inside the tube has to be a solution of a molybdenum[98] salt. The fluid should have a specific preferable properties. For example, for the atoms, other than molybdenum[98], a low neutron cross-section is desired, such that this does not influence the production by neutron capture by Molybdenum[98]. Unfortunately, the properties of such a solution are not easily found. So another fluid has to be used to test this model.

In this model the fluid is approximated as a simple sodium chloride solution, from which specific properties are known, such as the values of the specific heat capacity, the density and the thermal conductivity. However, the solubility of sodium chloride can be very different from the solubility of a molybdenum salt. The solubility of sodium molybdate is known [13], so this property is used.

# 3 Theory

The behavior of the system used in this thesis is dependent on different forces and properties, these will, among other things, be described in this section. First, the production of molybdenum[99] is discussed. Second, the dimensionless numbers used in this model are introduced, followed by the Boussinesq approximation. Next, the heat transfer inside the system is discussed. Then the heat generation is stated. Finally, the forces present in this system are introduced.

The total system is visualized in figure 4. In this figure, the gravity and friction forces are pictured. It can be seen that the friction is always in the opposite direction of the velocity and the gravity is in some tubes in the same direction and in some tubes in the opposite direction of the velocity.
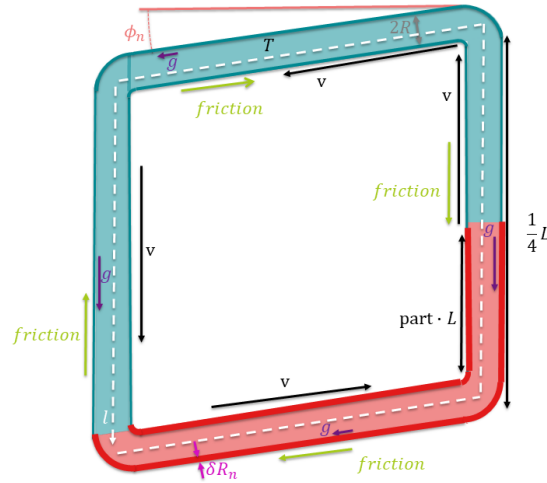


Figure 4: *A visualisation of the system, with $\delta R_n$ the thickness of the wall R the radius of the inner tube, v the velocity of the fluid inside the tube, $\phi_n$ the angle the pipe has with the x-axis, L the total length of the tube, $T_n$ the temperature of the fluid, g the gravitational force, friction the force caused by the friction and l the spatial coordinate along the length of the tube.*

## 3.1 Production

Production of molybdenum[99] will be obtained with neutron capture by molybdenum[98]. The production of molybdenum[99] can be calculated. This can be done by applying equation (3.1),

$$R = \frac{M_{Mo99}}{N_a} \Phi \sigma_{Mo98} N_{Mo98},  \tag{3.1}$$

with R the reaction rate of molybdenum in $\frac{\text{kg}}{\text{s}\,\text{m}^3}$, $M_{Mo99}$ the molar mass of molybdenum[99], $N_a$ the number of Avogadro, $\Phi$ the neutron flux in the HOR where the setup will be place, $\sigma_{Mo98}$ the neutron cross section of molybdenum[98] and $N_{Mo98}$ the number of molybdenum[98] atoms per volume. The last mentioned parameter has to be calculated by the expression shown in equation (3.2),

$$N_{Mo98} = \frac{N_a S}{M_{MoNa_2O_4}},  \tag{3.2}$$

in which $S$ is the solubility of sodium molybdate and $M_{MoNa_2O_4}$ is the molar mass of sodium molybdate.

## 3.2 Dimensionless numbers

In this thesis, dimensionless numbers will be used. The dimensionless numbers used in this model are Reynolds number, Prandtl number, Graetz number, Nusselt number, Grasshof number and

Rayleigh number. Each of these dimensionless numbers is discussed in this subsection.

- The Reynolds number is a measure of the ratio between the inertia forces and viscous forces. This term is also used to determine if a flow is classified as a laminar flow or a turbulent flow. Within a tube, the flow is considered laminar if the Reynolds number is lower than 2000 [4]. The Reynolds number is defined as in equation (3.3) [3],

$$\mathrm{Re} \equiv \frac{\rho d v}{\mu}, \tag{3.3}$$

with $\rho$ the density, $v$ the velocity, $\mu$ the dynamic viscosity and $d$ the characteristic length. Since the Reynolds number will only be used for the fluid inside the tube, the characteristic length for the Reynolds number here is the diameter of the inner tube, $2R$.

- The Prandtl number is a ratio between the momentum and thermal diffusivity [18]. Equation (3.4) is the definition of this dimensionless number [3],

$$\mathrm{Pr} \equiv \frac{\nu}{a}, \tag{3.4}$$

where $\nu = \frac{\mu}{\rho}$ is the kinematic viscosity and $a = \frac{\lambda}{\rho C_p}$ is the thermal diffusivity. Here $\lambda$ is the thermal conductivity and $C_p$ is the specific heat.

- The Graetz number is a ratio for conductive and convective heat transfer. The definition of this dimensionless number is described by equation (3.5) [3],

$$\mathrm{Gz} \equiv \frac{aL}{d^2 v}, \tag{3.5}$$

here $a$ is the thermal diffusivity, $L$ is the length in the transport direction, $d$ is the characteristic length and $v$ is the velocity. This dimensionless number is again used for only the fluid inside the tube, so this characteristic length is the diameter of the inner tube and the length in the transport direction is the length of the tube.

- The Nusselt number is a ratio between the total and the conductive heat transfer. This dimensionless number has the definition stated in equation (3.6) [3],

$$\mathrm{Nu} \equiv \frac{hd}{\lambda}, \tag{3.6}$$

with $\lambda$ the thermal conductivity, $d$ the characteristic length and $h$ the heat transfer coefficient. In the subsection about the heat transfer coefficient, this dimensionless number will be elaborated.

- The Grasshoff number describes the ratio between buoyancy and viscous forces. In this thesis, this dimensionless number is used to take the natural convection outside of the tube into account in the heat transfer coefficient. The expression of this number in this case is described in equation (3.7) [3],

$$\mathrm{Gr} \equiv \frac{d^3 g \beta |T_B - T_\infty|}{\nu^2}, \tag{3.7}$$

in which $d$ is again the characteristic length, $g$ is the gravitational constant, $\beta$ is the thermal expansion coefficient, $T_B$ is the temperature of the wall and $T_\infty$ is the temperature of the surrounding water. The characteristic length, $d$ will be the vertical length, so for the vertical tube the length of this part of the tube, $\frac{1}{4}L$, is the characteristic length and for the horizontal part of the tube the characteristic length will be the diameter of the tube, $2R + 2\delta R$.

- The Rayleigh number is the ratio between the natural convective and the diffusive heat transfer [19]. The expression used for this dimensionless number is stated in equation (3.8),

$$\mathrm{Ra} = \mathrm{Gr} \cdot \mathrm{Pr}, \tag{3.8}$$

in which Gr and Pr are the previously mentioned dimensionless numbers.

## 3.3 Boussinesq approximation

The movement of the fluid is dependent on natural convection, and so dependent on the variation of the density inside the system. This means that there can not be assumed that everywhere in the derivation the density remains constant. Therefore, the Boussinesq approximation will be used, which can only be applied if the density only depends on the temperature and if the variation of the density in the system is not too large [5]. This approximation states that the variation of the density only has to be taken into account for the gravitational forces [5]. So in this system, the density $\rho_0$, will be taken as a fixed reference density. However, the density will be dependent on the temperature for the gravitational part.

## 3.4 Heat Transfer inside the system

Newton's law of cooling, see equation (3.9), will be used. This means that the heat transfer coefficients are needed.

$$\phi_{q_{D_1 D_2}} = h_{D_1 D_2} A_{D_1 D_2} (T_{D_2} - T_{D_1}),$$
$$\text{with} \tag{3.9}$$
$$h_{D_1 D_2} = (h_{D_1}^{-1} + h_{D_2}^{-1})^{-1}.$$

In equation (3.9) a system is considered of two regions $D_1$ and $D_2$ with an area $A_{D_1 D_2}$, which connect this regions. The energy flow from region $D_1$ to region $D_2$ is $\phi_{q_{D_1 D_2}}$. The heat transfer coefficient inside region $D_1$ is $h_{D_1}$ and the heat transfer coefficient inside region $D_2$ is $h_{D_2}$. The temperature in region $D_1$ is $T_{D_1}$ and the temperature in region $D_2$ is $T_{D_2}$.

The heat transfer coefficients needed to model this system are the heat transfer coefficient inside the fluid inside the tube, inside the wall of the pipe and inside the surrounding water. The visualization of this system can be seen in figure 5, here the fluid inside the tube is taken as region $A$, the wall as region $B$ and the surrounding water as region $C$.
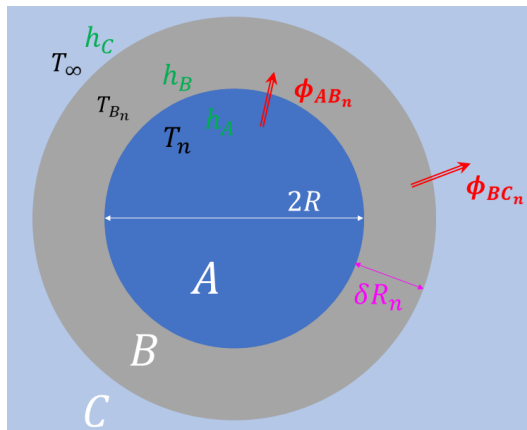


Figure 5: *An intersection of the tube, with $h_A$ the heat transfer coefficient inside region $A$, $h_B$ the heat transfer coefficient inside region $B$, $h_C$ the heat transfer coefficient inside region $C$, $T_n$ the temperature of region $A$, $T_{B_n}$ the temperature of region $B$, $T_\infty$ the temperature of region $C$, $\phi_{AB_n}$ the energy flow from region $A$ to region $B$, $\phi_{BC_n}$ the energy flow from region $B$ to region $C$, $R$ the radius of the inner tube and $\delta R$ the thickness of region $B$.*

The expression for the heat transfer coefficient is described in equation (3.10), which is also stated in a different form in the subsection dimensionless numbers,

$$h = \frac{\text{Nu}\lambda}{d}, \tag{3.10}$$

with Nu the Nusselt number, $\lambda$ the thermal conductivity and $d$ the characteristic length.

### 3.4.1 Heat transfer coefficient inside the fluid inside the tube

First, the heat transfer coefficient inside the fluid inside the tube will be described. The characteristic length $d$, here is the diameter of the pipe $2R$. For the Nusselt number equation (3.11) is used [3],

$$\text{Nu} = \begin{cases} 0.027\text{Re}^{0.8}\text{Pr}^{0.33}, & \text{Re} > 10^4 \text{ \& Pr} \geq 0.7, \\ 1.62\ \text{Gz}^{-1/3}, & \text{Gz} < 0.05 \text{ \& Re} < 2000, \\ 3.66, & \text{Gz} > 0.1 \text{ \& Re} < 2000. \end{cases} \tag{3.11}$$

In which the following dimensionless numbers are used, Reynolds number Re, Prandtl number Pr and Greatz number Gz. To calculate the heat transfer coefficient, the equation (3.10) will be used, with the characteristic length being the diameter inside the tube. The dimensionless numbers used in this expression are independent on the location in the system, so the heat transfer coefficient of the fluid inside the tube is independent on the location inside the tube.

### 3.4.2 Heat transfer coefficient inside the wall

However, the heat transfer coefficient inside the wall does depend on the location of the tube. This is because it is dependent on the thickness of the tube, since the characteristic length $d$, is the thickness of the wall $\delta R$. For the heat transfer coefficient inside the wall equation (3.12) is be used [4], here the wall is approximated to be an one-dimensional wall.

$$h = \frac{\lambda}{\delta R}. \tag{3.12}$$

### 3.4.3 Heat transfer coefficient inside the surrounding water

The heat transfer coefficient inside the water outside the tube will be more complicated. The water outside the pipe does not have a velocity at the beginning, so initially this water stands still, this means that the water will be heated. So the density of the water will change what results in natural convection around the outside of the pipe, causing a velocity of the surrounding water around the pipe.

The natural convection in the water surrounding the pipe will have different effects at different location in the system. Since the density will drop, the heated water will move up in the vertical direction. So this will have a different effect on the horizontal and vertical part of this system. In the horizontal part, the water will move around the pipe in an upward direction, while in the vertical part the water will move along the pipe in the vertical direction. To have a better overview of this situation, see figure 6.
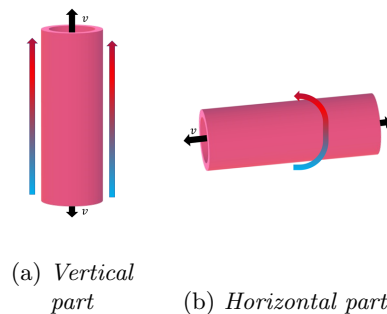


(a) *Vertical part*  (b) *Horizontal part*

Figure 6: *Natural convection around the pipe*

In figure 6a it can be seen that the heated water outside the tube moves in the same or opposite direction of the fluid inside the tube. Since the energy transport in the vertical tube is dependent on the temperature of the surrounding water, it has to be taken into account that the water in the

top part of the tube has a higher temperature than in the bottom part of the tube. To take this factor into account, the heat transfer coefficient has to be changed for the surrounding water in the vertical part of the system. From Xian et al. [7] the expression for the Nusselt number in this case is obtained, described in equation (3.13),

$$\text{Nu} = \frac{4}{3}\text{Ra}^{0.25}\left(\frac{7\text{Pr}}{100 + 105\text{Pr}}\right)^{0.25} + \frac{4}{35}\frac{272 + 315\text{Pr}}{64 + 63\text{Pr}}\frac{\frac{1}{4}L}{2(R + \delta R)}. \tag{3.13}$$

This expression is valid for the following values, $10^8 < \text{Gr} < 4 \cdot 10^9$ [19]. But in this system the values $\text{Gr} < 10^8$ can also occur, so another equation to describe the nusselt number when $\text{Gr} < 10^8$ is needed. For this a more general equation, also provided by Xian et al. [7], is stated in equation (3.14),

$$\text{Nu} = 0.48\text{Ra}^{0.25} \tag{3.14}$$

Equation (3.14) can be used in the region $10^4 < \text{Ra} < 10^9$. The characteristic length $d$, used to calculate the heat transfer coefficient in the vertical part is the length of the vertical pipe $\frac{1}{4}L$.

In figure 6b it can be seen that the natural convection has another effect on the horizontal tube. In this case, the surrounding water seems to be moving in almost the perpendicular direction to the flow of the fluid inside the tube. Thus, it is obvious that not the same correlation for the Nusselt number as in the vertical part can be used. Since the angle in this system is very small, it will be assumed to be zero for this calculation of the heat transfer coefficient. With this approximation the expression described in equation (3.15) can be used [19],

$$\text{Nu} = \left(0.6 + \frac{0.387\text{Ra}^{\frac{1}{6}}}{\left(1 + \frac{0.559^{\frac{9}{16}}}{\text{Pr}}\right)^{\frac{8}{27}}}\right)^2. \tag{3.15}$$

This equation is usable for a wide range of values of the Rayleigh number, $10^{-5} < \text{Ra} < 10^{12}$. The characteristic length used to calculate the heat transfer coefficient in the horizontal part is the diameter of the tube $2(R + \delta R)$.

## 3.5 Heat generation

Heat is generated inside the wall of the tube, this is due to absorption of gamma radiation. The quantity of production of this energy is dependent on the volume of the wall. Equation (3.16) can be used to determine the energy production in the wall with volume $V_{wall}$ [19],

$$P_\gamma = u\rho_{wall}V_{wall}, \tag{3.16}$$

in which $\rho_{wall}$ is the density of the wall, $P_\gamma$ is the heat generated in the wall and $u$ is the heating generation per mass material. For the last parameter the following value is used, $u = 300\frac{\text{W}}{\text{kg}}$ [19]. As stated before this heat generation is dependent on the thickness of the wall, which will be different at different spatial coordinates $l$, inside the system. This is because the heat generation is dependent on the mass, which is in its turn dependent on the thickness of the wall. Equation (3.17) is the expression for the volume of a part of the wall with thickness $\delta R_1$ and length $L_1$,

$$V_{wall_1} = \pi L_1((R + \delta R_1)^2 - R^2). \tag{3.17}$$

## 3.6 Forces

In figure 4 two different forces are visualized, the gravitational force and the friction force. The gravitational force is responsible for the natural convection in the system combined with the change of the density in the system. This force can later be seen as a term in the derivation of the velocity. The velocity is assumed to be constant over the length of the tube, this is done since the radius of the tube will also be taken constant.

The friction force can be divided into two parts, friction due to the wall and friction due to the bends in the tube. Both these frictions are later implemented in the derivation for the velocity as terms for the pressure drop.

### 3.6.1 Friction due to the wall

The friction of the wall is described by the pressure drop in the system as equation (3.18) [5],

$$\left(\frac{dp}{dl}\right)_{\text{friction of wall}} = -f_D \frac{1}{2R}\left(\frac{1}{2}\rho_0 v^2\right), \tag{3.18}$$

with $f_D$ the Darcy friction factor, $R$ the radius of the tube, $\rho_0$ the fixed reference density of the fluid and $v$ the velocity of the fluid. The Darcy friction factor is dependent on the Reynolds number. An expression for this factor is given by Vasilis et al. [8] valid for both the laminar and turbulent regime, which is stated in equation (3.19),

$$f_D = \left(\frac{64}{\text{Re}}\right)^2 \left(0.75\ln\left(\frac{\text{Re}}{5.37}\right)\right)^{2(\alpha-1)b}\left(0.88\ln\left(3.41\frac{2R}{\epsilon}\right)\right)^{2(\alpha-1)(1-b)},$$

with

$$\alpha = \frac{1}{1+\left(\frac{\text{Re}}{2712}\right)^{8.4}} \qquad \text{and} \qquad b = \frac{1}{1+\left(\frac{\text{Re}}{150\frac{2R}{\epsilon}}\right)^{1.8}}. \tag{3.19}$$

In this equation for the Darcy friction, $R$ is the radius of the tube and $\epsilon$ the height of the roughness, also known as the effective roughness.

### 3.6.2 Friction due to bends

The pressure loss due to the bends in the loop is also known as the local pressure loss. This system has four bends, the four corners. Two of these corners have an angle of $90^o - \phi$ degrees and the other two have an angle of $90^o + \phi$ degrees. Since this angle, $\phi$, will be taken very small the corners will be approximated to have an angle of $90^o$ degrees for the calculation of the contribution of the corners to the pressure drop. For this pressure loss an expression is known, which is stated in equation (3.20) [5],

$$\left(\frac{dp}{dl}\right)_{\text{local}} = -\kappa(\frac{1}{2}\rho_0 v^2)\delta(l), \tag{3.20}$$

with $\kappa$ the friction coefficient, $\rho_0$ the fixed reference density, $v$ the velocity of the fluid and $\delta(l)$ the delta function at position $l$. So in this case there are 4 different none zero points since there are four corners. The friction coefficient for $90^o$ degrees corner is the following $\kappa = 1.30$.

# 4 Methods

In this section, first the discretization used later on is described. Secondly, the equations in which the temperature and velocity are expressed are derived for the three methods. Lastly, the time dependent method, the time independent method and the time independent analytical method will be described.

## 4.1 Discretization

For this model, the system has to be discretized. This discretization has to be done for both numerical methods and also for the numerical determination of the velocity for the analytical method, both of these methods will be described later in this section.

For the discretization, $N$ segments will be taken of equal length. Each part of the tube will have the same number of segments and a segment will not be within multiple parts of the tube. Thus the number of segments, $N$, has to be divisible by four. These segments are visualized in figure 7. One segment is the region between two black lines.
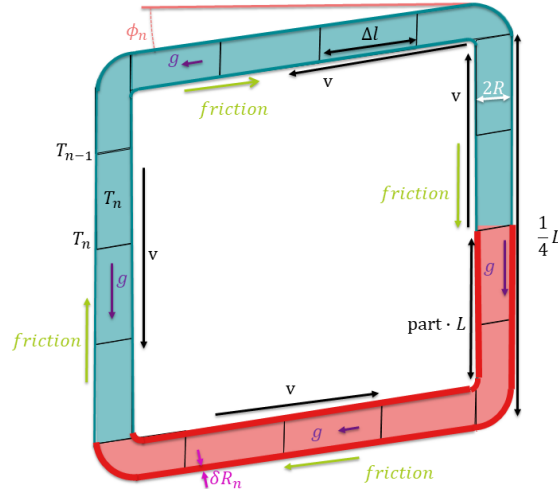


Figure 7: *Visualization of the system, with $\delta R_n$ the thickness of the wall in segment $n$, $R$ the radius of the inner tube, $v$ the velocity of the fluid inside the tube, $\phi_n$ the angle the pipe in segment $n$ has with the x-axis, $L$ the total length of the tube, $\Delta l$ the length of a segment, $T_n$ the temperature of the fluid inside the tube in segment $n$, $g$ the gravitational force and friction the force caused by the friction.*

## 4.2 Internal energy

The energy balance is described in the equation (4.1) [5],

$$\rho C_p \frac{DT}{Dt} = q''' - \nabla q'' + T \frac{DP}{Dt} + \bar{\bar{\tau}} : \nabla \boldsymbol{v}. \tag{4.1}$$

In equation (4.1) the term on the left hand side contains the accumulation and convective transport term in which the first term is the derivative with respect to time and the second term is the derivative with respect to the spacial coördinates times the velocity in that specific direction. The first term on the right hand side is the heat production inside the system. The second term is the conductive transport, so the conduction term. Followed by the third term which is the term connected to the pressure changes. And lastly, the fourth term represents the dissipation due to friction.

Fourier's law is used in this derivation and the following approximations are used. The influence of the pressure changes on the energy is assumed to be negligible, so $\frac{DP}{Dt} = 0$. Also this model approximate the influence on the energy by friction to be zero, so $\bar{\bar{\tau}} : \nabla v = 0$. For this system, it will be useful to work in cylindrical coordinates, since the system is a cylindrical shaped pipe. The temperature in two different regions will be used: the temperature of the wall and the temperature of the fluid inside the tube.

The velocity of the fluid will be considered to be in the direction of the spatial coordinate $l$. This model neglects the heat production caused by the neutron capture inside the fluid. Equation (4.2) is obtained for the temperature of the fluid in the tube.

$$\rho_0 C_p \left( \frac{\partial T}{\partial t} + v \frac{\partial T}{\partial l} \right) = k \left( \frac{1}{r} \frac{\partial}{\partial r} \left( r \frac{\partial T}{\partial r} \right) + \frac{1}{r^2} \frac{\partial^2 T}{\partial \theta^2} + \frac{\partial^2 T}{\partial l^2} \right), \tag{4.2}$$

with $\rho_0$ the fixed density of the fluid, $T$ the temperature of the fluid, $v$ the velocity of the fluid within the tube and $C_p$ the specific heat of the fluid.

In the wall region heat production due to gamma radiation is present. Also, the velocity in all directions can be taken to be zero, since the material is in solid state. So for this region equation (4.3) is valid,

$$\rho_{wall} C_{p_{wall}} \frac{\partial T_B}{\partial t} = q''' + k \left( \frac{1}{r} \frac{\partial}{\partial r} \left( r \frac{\partial T_B}{\partial r} \right) + \frac{1}{r^2} \frac{\partial^2 T_B}{\partial \theta^2} + \frac{\partial^2 T_B}{\partial l^2} \right), \tag{4.3}$$

with $\rho_{wall}$ the density of the wall, $T_B$ is the temperature of the wall and $C_{p_{wall}}$ the specific heat of the wall.

### 4.2.1 Numerical time dependent method, temperature of the fluid

First, the fluid region in this system will be considered. This model assumes the velocity is constant over the length in the tube, since the tube does not change in radius over the length and the changes in density are relatively small. This last one otherwise causes the velocity to be changed throughout the length of the tube. When the density is at a certain location high relatively to other locations this high density causes a lower velocity since the fluid has "shrunken" at this location.

For the discretized system it will be approximated that the temperature inside a segment is the same as the temperature that flows out of the segment. When discretising and integrating over one segment in the loop equation (4.4) is obtained,

$$\rho_0 C_p \pi R^2 (l_n - l_{n-1}) \frac{\partial T_n}{\partial t} + (T_n - T_{n-1}) \rho_0 C_p \pi R^2 v = -\phi_{q_{AB_n}}, \tag{4.4}$$

with $(l_n - l_{n-1}) = \Delta l = L/N$ the length of a segment, taking all the segments with equal length. $T_n$ is the temperature of the fluid in segment n, $N$ is the total number of segments in the system, $R$ is the radius of the inner tube and $\phi_{q_{AB_n}}$ $(= A_{AB} k \frac{dT}{dr})$ the heat loss or gain over the surface of the region by conduction through the surroundings of the region [4]. In this case, this is the heat which goes to the wall. With Newton's law of cooling described in equation (3.9) the heat transport from the fluid to the wall $\phi_{q_{AB_n}}$, can be determined by equation (4.5),

$$\phi_{q_{AB_n}} = h_{AB_n} A_{AB} (T_n - T_{B_n}),$$
$$\text{with} \tag{4.5}$$
$$h_{AB_n} = (h_A^{-1} + h_{B_n}^{-1})^{-1}.$$

In equation (4.5) there are multiple parameters, $A_{AB}$ which is the surface between the fluid and the wall and $T_{B_n}$ which is the temperature of the wall in segment n. Also stated in equation (4.5) are the heat transfer coefficients $h_A$ and $h_B$ for the fluid and the wall, respectively. The heat transfer coefficient of the fluid is dependent on the velocity. The heat transfer coefficient of the wall is dependent on the thickness of the wall, so this is dependent on the location inside the tube. The surface between the fluid and the wall in each segment is $A_{AB} = \frac{L}{N} 2\pi R$.

So for this time dependent problem equation (4.6) is used in the Runga Kutta method,

$$\frac{\partial T_n}{\partial t} = -\frac{2h_{AB_n}}{R\rho_0 C_p}(T_n - T_{B_n}) - \frac{N}{L}(T_n - T_{n-1})v. \tag{4.6}$$

Equation (4.6) is the expression for the derivative of the temperature in segment $n$ with respect to time, this equation consists of two parts. The first part is responsible for the heat transfer from the fluid to the wall and the second part is responsible for convection.

### 4.2.2 Numerical time dependent method, temperature of the wall

Now an equation for the temperature of the wall will be derived. Also for this derivation, the discretization of the system is needed. Again by integrating over one segment, an equation is obtained, which is shown in equation (4.7),

$$\rho_{wall} V_{wall_n} C_{p_{wall}} \frac{\partial T_{B_n}}{\partial t} = V_{wall_n} q''' + \phi_{q_{AB_n}} - \phi_{q_{BC_n}}, \tag{4.7}$$

with $V_{wall_n} = \pi \frac{L}{N}((R + \delta R_n)^2 - R^2) = \pi \frac{L}{N}(2 R \delta R + \delta R_n^2)$, from which $\delta R_n$ the thickness of the wall is in segment $n$.

In this equation (4.7) $V_{wall_n}$ is the volume of the wall in segment n, $\phi_{q_{AB_n}}$ is the heat transfer from the fluid to the wall and $\phi_{q_{BC_n}}$ is the heat transfer from the wall to the surrounding water outside the tube. The heat generation is due to gamma radiation, for which the following is known, $q''' = u \rho_{wall}$ with $u$ the heat generation per mass. This heat generation is described in equation (3.16).

Again Newton's law of cooling equation (4.8) is used to determine the heat transfer from the wall to the surrounding water $\phi_{q_{BC_n}}$,

$$\phi_{q_{BC_n}} = h_{BC_n} A_{BC_n} (T_{B_n} - T_C)$$
$$\text{with}$$
$$h_{BC_n} = (h_{B_n}^{-1} + h_{C_n}^{-1})^{-1}.$$

$$(4.8)$$

In equation (4.8) the parameter $A_{BC_n} = \frac{L}{N} 2\pi(R + \delta R_n)$ is the surface between the wall of the tube and the surrounding water in segment n and $T_c$ is the temperature of the surrounding water. Also the heat transfer coefficient $h_B$ and $h_C$ for the wall and the surrounding water respectively, are present in equation (4.8). The heat transfer coefficient of the surrounding water is dependent on the diameter of the tube and the temperature of the wall, which makes this also location dependent. Equation (4.9) is obtained, by combining equations (4.7) and (4.8), which can be used in the Runga Kutta method,

$$\frac{\partial T_{B_n}}{\partial t} = \frac{u}{C_{p_{wall}}} + \frac{2h_{AB_n}}{C_{p_{wall}}\rho_{wall}} \frac{R}{2R\delta R_n + \delta R_n^2}(T_n - T_{B_n}) - \frac{2h_{BC_n}}{C_{p_{wall}}\rho_{wall}} \frac{(R + \delta R_n)}{2R\delta R_n + \delta R_n^2}(T_{B_n} - T_C).$$

$$(4.9)$$

Equation (4.9) is the expression for the derivative of the temperature of the wall in segment $n$ with respect to time, this equation consists of three parts. The first term is to take the heating inside the wall due to the gamma radiation into account. The second term is again responsible for the heat transfer from the fluid to the wall. Lastly, the third term is responsible for the heat transfer from the wall to the surrounding water.

### 4.2.3 Numerical time independent method, temperature of the fluid and the wall

Looking at the time independent problem the derivatives to time are set equal to zero, $\frac{\partial T_{B_n}}{\partial t} = \frac{\partial T_n}{\partial t} = 0$, so equations (4.10) are used to describe segment n,

$$0 = -\frac{2h_{AB_n}}{R\rho_0 C_p}(T_n - T_{B_n}) - \frac{N}{L}(T_n - T_{n-1})v,$$

$$0 = \frac{u}{C_{p_{wall}}} + \frac{2h_{AB_n}}{C_{p_{wall}}\rho_{wall}} \frac{R}{2R\delta R_n + \delta R_n^2}(T_n - T_{B_n}) - \frac{2h_{BC_n}}{C_{p_{wall}}\rho_{wall}} \frac{(R + \delta R_n)}{2R\delta R_n + \delta R_n^2}(T_{B_n} - T_C).$$

$$(4.10)$$

Rewriting equations (4.10), an expression for the temperature of the fluid and for the temperature of the wall both in segment n are given in equations (4.11),

$$T_n = \left(\frac{2h_{AB_n}}{R\rho_0 C_p} + \frac{N}{L}\right)^{-1}\left(\frac{2h_{AB_n}}{R\rho_0 C_p}(T_{B_n}) + \frac{N}{L}(T_{n-1})v\right),$$

$$T_{B_n} = \left(h_{AB_n}\frac{R}{R + \delta R_n} + h_{BC_n}\right)^{-1}\left(\frac{1}{2}\rho_{wall}u\frac{(2R + \delta R_n)\delta R_n}{R + \delta R_n} + h_{AB_n}\frac{R}{R + \delta R_n}T_n + h_{BC_n}T_C\right).$$

$$(4.11)$$

Equations (4.11) will be used for the steady state numerical approach.

### 4.2.4 Analytical time independent method, temperature of the fluid

For the analytical method the steady state is taken, this means that the derivative with respect to time is zero. So equation (4.12) is gotten for the temperature for the fluid when there is integrated over the angle $\theta$ and the radius $r$,

$$\pi R^2 \rho_0 C_p \left( v \frac{\partial T(l)}{\partial l} \right) = -\frac{\partial \phi_{q_{AB_n}}(l)}{\partial l}. \tag{4.12}$$

Since the system is in steady state the energy generated in the wall by gamma heating, $u\rho_{wall}V_{wall}$, is equal to the energy which leaves the wall. The energy that leaves the wall is described by $\phi_{q_{BC}}$ and $-\phi_{q_{AB}}$, these are relatively the energy which leaves the wall to the surrounding water and the energy which leaves the wall to the fluid inside the tube. Thus the expression stated in equation (4.13) is obtained,

$$u\rho_{wall}V_{wall}(l) = \phi_{q_{BC}}(l) - \phi_{q_{AB}}(l). \tag{4.13}$$

The expression for the energy flow from the wall to the surrounding water is known, combining equations (4.13) and (4.8) an expression for the energy flow from the fluid inside the tube to the wall is obtained, this is described in equation (4.14),

$$\phi_{q_{AB}}(l) = h_{BC} A_{wall_{\Delta l}} (T_B(l) - T_C) - u\rho_{wall}V_{wall}(l). \tag{4.14}$$

The energy flow described in equation (4.14) is the energy flow from the wall to the fluid over a certain domain. So the derivative of this energy flow with respect to the spatial coordinate $l$ is described as in equation (4.15),

$$\frac{\partial \phi_{q_{AB}}(l)}{\partial l} = h_{BC} 2\pi (R + \delta R(l))(T_B(l) - T_C) - u\rho_{wall}\pi((R + \delta R(l))^2 - R^2). \tag{4.15}$$

Combining equation (4.15) and the earlier obtained equation (4.12), there will be the ordinary differential equation described in equation (4.16) which is dependent on the location in the system $l$ and the temperature profile of the wall,

$$\pi R^2 \rho_0 C_p \left( v \frac{\partial T(l)}{\partial l} \right) = -h_{BC} 2\pi (R + \delta R(l))(T_B(l) - T_C) + u\rho_{wall}\pi((R + \delta R(l))^2 - R^2). \tag{4.16}$$

To solve equation (4.16) an expression for the temperature in the wall must be obtained. The remaining ordinary differential equation can be solved by dividing the loop into four regions. For each of these regions, a solution is found with different constants. The complete derivation is stated in the appendix B. Equation (4.17) is obtained for the temperature of the fluid inside the tube for the analytical model,

$$\begin{cases} T(l) = \sum_{n=1}^{4} \left( -\frac{B_n}{A_n} + \alpha_n e^{A_n l} \right) \mathbb{1}_{[L_{n-1}, L_n]}(l), \\[2em] \text{with} \quad B_n = \frac{h_{AB_n} \, \delta R_n \, (2R + \delta R_n) \, u \, \rho_{wall} + 2 h_{AB_n} \, h_{BC_n} \, (R + \delta R_n) \, T_C}{v \, R \, \rho_0 \, C_p \, (h_{AB_n} R + h_{BC_n} (R + \delta R_n))}, \\[2em] A_n = \frac{-h_{BC_n} \, h_{AB_n} \, 2(R + \delta R_n)}{v \, R \, \rho_0 \, C_p \, (h_{AB_n} R + h_{BC_n} (R + \delta R_n))}, \end{cases} \tag{4.17}$$

with $\mathbb{1}(l)$ the indicator function, the definition of this function is stated in appendix B. The constant $\alpha_n$ in equation (4.17) is also defined in appendix B.

## 4.3  Velocity

From the three dimensional Navier Stokes equation for newtonian fluids and from assuming that the velocity inside the tube will be constant over the spatial coordinate $l$ of the tube, an expression for the derivative of the velocity with respect to time can be obtained, which is stated in equation (4.18),

$$\rho \frac{\partial v}{\partial t} = -\frac{\partial P}{\partial l} + \rho g \sin(\phi), \tag{4.18}$$

in which the friction is included in the pressure derivative, the first term on the right hand side. The derivation from the Navier Stokes equation to equation (4.18) is stated in the appendix.

### 4.3.1  Numerical methods, velocity

For the numerical method, both the time independent and the time dependent system will be looked into. Firstly, for the time dependent system equation (4.18) is used.
After integrating the equation over the whole region, equation (4.19) is obtained,

$$\int \rho_0 \frac{\partial v}{\partial t} dl = -\int \frac{\partial P}{\partial l} dl + \int \rho g \sin(\phi) dl. \tag{4.19}$$

This model assumes that the change in density is only important for the gravitational force integral as stated earlier in the subsection about the Boussinesq approximation. The pressure derivative will be split into three parts, the friction part, the local changes part and the internal pressure changes part. When these parts are implemented in the previous equation (4.19) the new equation (4.20) is found [5],

$$\int \rho_0 \frac{\partial v}{\partial t} dl = \int \left( \frac{\partial P_{internal}}{\partial l} - f_D \frac{\frac{1}{2}\rho_0}{D} v^2 - \kappa(\frac{1}{2}\rho_0 v^2)\delta(l) \right) dl + \int \rho g \sin(\phi_l) dl, \tag{4.20}$$

with $D = 2R$ the diameter of the inner tube, $f_D$ the Darcy friction, $g$ the gravitational constant, $\phi$ the angle position of the tube with respect to the z-axis, $\rho_0$ the fixed density of the fluid, $\rho$ the temperature dependent density of the fluid and $\kappa$ the friction coefficient for flow through sudden changes in the tube system, bends for example.

In equation (4.20) the first integral of the right hand side is the term to take the pressure changes into account, these integral is divided into three terms. The first of these three terms is responsible for the internal pressure changes, the second term is for the pressure changes due to friction and the last term is the term describing the local pressure changes due to the bends of the tube in the system. From the discretization of equation (4.20) follows equation (4.21), which describes the momentum balance in segment $n$,

$$\rho_0 \frac{\partial v}{\partial t} \Delta L = \Delta P_{internal} - f_{D_n} \frac{\rho_0}{4R} \Delta L v^2 - \rho_0 v^2 \frac{1}{2}((\mathbb{1}_{L_1} + \mathbb{1}_{L_3})\kappa_1 + (\mathbb{1}_{L_2} + \mathbb{1}_{L_4})\kappa_2) + g\Delta L \rho_n \sin(\phi_n). \tag{4.21}$$

Equation (4.21) will be summed over the N segments. Due to the indicator function present in equation (4.21), $\rho_0 v^2(\kappa_1 + \kappa_2)$ remains for the third term on the right hand side. The internal pressure term will fall out and equation (4.22) remains,

$$\rho_0 \frac{\partial v}{\partial t} L = -\sum_{n=1}^{N} f_{D_n} \frac{\rho_0}{4R} \Delta L v^2 - \rho_0 v^2(\kappa_1 + \kappa_2) + g\Delta L \sum_{n=1}^{N} \rho_n \sin(\phi_n). \tag{4.22}$$

The density is dependent on the temperature, from the Boussinesq approximation equation (4.23) is used,

$$\rho = \rho_0 - \rho_0 \beta(T - T_0), \tag{4.23}$$

with $\beta$ the Thermal expansion coefficient [5]. So the equation for the velocity of the time dependent numerical part used will be as described in equation (4.24),

$$\frac{\partial v}{\partial t} = -\frac{1}{N}\sum_{n=1}^{N} f_{D_n}\frac{1}{4R}v^2 - \frac{v^2}{L}(\kappa_1 + \kappa_2) + \frac{g}{N}\sum_{n=1}^{N}(1 - \beta(T - T_0))\sin(\phi_n). \qquad (4.24)$$

This equation can be used for the Runga Kutta method.

For the time independent part, which is for a steady state, the derivative with respect to time is zero, $\frac{\partial v}{\partial t} = 0$. Implementing this and rewriting equation (4.24) an expression for the velocity is again found, stated in equation (4.25),

$$v = \sqrt{\frac{\frac{g}{N}\sum_{n=1}^{N}(1 - \beta(T - T_0))\sin(\phi_n)}{\frac{1}{N}\sum_{n=1}^{N} f_{D_n}\frac{1}{4R} + \frac{1}{L}(\kappa_1 + \kappa_2)}}. \qquad (4.25)$$

Equation (4.25) will be used for the steady state numerical method.

### 4.3.2 Analytical time independent method, velocity

For the analytical method there will only be looked into a steady state system, this means the derivatives with respect to time will be zero, $\frac{\partial v}{\partial t} = 0$. So the right hand side of equation (4.18) is equal to zero.

In this equation, the pressure over the length is dependent on different properties, in this thesis for the analytical method two of these properties are taken into account, namely, the pressure differences due to friction and due to local changes in the pipe. Then equation (4.26) is obtained,

$$0 = -f_D\frac{\rho_0}{4R}v^2 - \kappa(\frac{1}{2}\rho_0 v^2)\delta(l) + \rho g\sin(\phi_l), \qquad (4.26)$$

with $f_D$ the Darcy friction, $\rho_0$ the fixed reference density, $R$ the radius of the tube, $v$ the velocity of the fluid, $\kappa$ the friction coefficient, $\delta(l)$ the delta function at position l, $\phi$ the angle position of the tube with respect to the z-axis and $g$ the gravitational constant.

For the analytical method, the equation will be integrated over the region. Since in this system there are four different angles of the gravitational force applied relative to the velocity, this integral can be divided into four different integrals with constant angles. Equation (4.23) can again be used in this derivation. Applying these steps and after rewriting equation (4.27) follows,

$$\begin{cases} v = \left(\sum_{n=1}^{4} C_n \int_{L_{n-1}}^{L_n} T(l)dl\right)^{1/2}, \\ C_n = \frac{-g\beta\sin(\phi_n)}{f_D\frac{1}{4R}L + (\kappa_1 + \kappa_2)}. \end{cases} \qquad (4.27)$$

Equation (4.27) will be used in the analytical method. The derivation of the velocity is implemented in the appendix.

## 4.4 Numerical methods

In this thesis, two different numerical methods are used. For the time dependent model, the Runga Kutta method is used. For the time independent model, the Newton-Raphson method is used. First, the time dependent method will be discussed in this subsection. After that, the time independent method is explained.

### 4.4.1 Time dependent model

The purpose of the time dependent model is mainly to see if this model will go towards a steady state. The results of this time dependent method will also be used as an initial guess needed in the time independent method. The equations needed for this model are stated in subsections, 4.2.2, 4.2.1 and 4.3.1. These equations are equation (4.24), (4.4) and (4.9). These are three ordinary differential equations. So a system described in equation (4.28) is obtained.

$$f_1 = \frac{dv}{dt}, \qquad f_2 = \frac{dT}{dt}, \qquad f_3 = \frac{dT_b}{dt}. \tag{4.28}$$

A well-known numerical method for this time dependent problem is the Runga Kutta method. In this thesis, the fourth order Runga Kutta method is used, which has a local truncation error of $\mathcal{O}(\Delta t^4)$ [6]. Equation (4.29) is the method that approximate the solution at the next time step from the Runga Kutta method, this is based on the Simpson's rule for numerical integration [6],

$$w_{n+1} = w_n + \frac{1}{6}(k_1 + 2k_2 + 2k_3 + k_4),$$
$$\text{with}$$
$$k_1 = \Delta t f(t_n, w_n),$$
$$k_2 = \Delta t f(t_n + \frac{1}{2}\Delta t, w_n + \frac{1}{2}k_1),$$
$$k_3 = \Delta t f(t_n + \frac{1}{2}\Delta t, w_n + \frac{1}{2}k_2),$$
$$k_2 = \Delta t f(t_n + \Delta t, w_n + k_3),$$

$$\tag{4.29}$$

in which $t_n$ is the time at step $n$, $\Delta t$ is the step size used and $w_n$ is the solution found in step $n$. In this case, the parameter $w$ is a vector of the velocity, the temperatures of the fluid in each segment and the temperatures of the wall in each segment. The function $f$ is in this case also a vector constructed by the functions stated in equation (4.28).

For the first time step of this method, an initial condition is needed. Since this system contains a division by Reynolds number, which is zero when the velocity is zero, the initial condition for the velocity can not be zero in this model. The initial condition used in this thesis will be given in the results section of this thesis.

A Python code will be constructed to apply the Runga Kutta method. This Python code can be found via appendix A. The structure of this code is visible in figure 8.
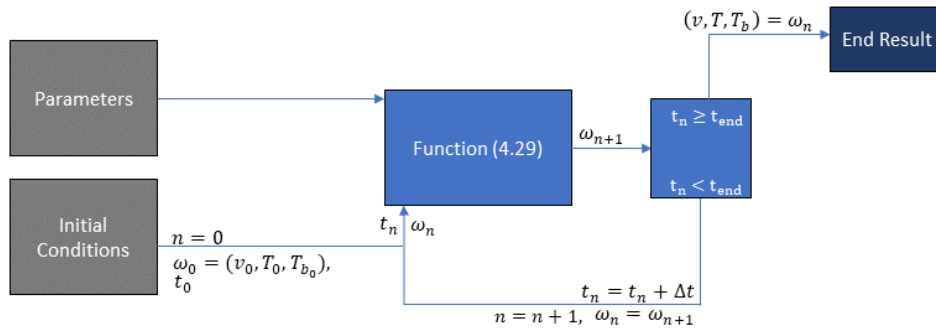


Figure 8: *Method of solving the time dependent numerical system.*

### 4.4.2  Time independent method

If the time dependent model shows that this system does have a steady state, the time independent method can be used. This method will be used to directly determine the equilibrium of the system and analyze its behavior under variations of different properties, such as using different proportions. The equations used in this method are derived in subsections 4.2.3 and 4.3.1, these are equations (4.25) and (4.11). For this method, the Newton Raphson method will be used. For the Newton Raphson method a system is needed of the form $\mathbf{g}(\mathbf{x}) = \mathbf{0}$. The function $\mathbf{g}$ is again a vector of functions, which contains equations (4.25) and (4.11) rewritten to a function of the form $g_i(\mathbf{x}) = 0$. Furthermore, the following variables are again combined in a vector $\mathbf{x}$, the velocity, the temperature of the fluid in each segment and the temperature of the wall in each segment.

Now the correct form is obtained to apply the Newton Raphson method, which is described in equation (4.30) [6],

$$\mathbf{x}_n = \mathbf{x}_{n-1} - \mathbf{J}^{-1}(\mathbf{x}_{n-1})\mathbf{g}(\mathbf{x}_{n-1}), \tag{4.30}$$

with $\mathbf{x}_n$ the solution of the nth iteration and $\mathbf{J}(\mathbf{x}_{n-1})$ the jacobian of $\mathbf{g}$ at $\mathbf{x}_{n-1}$.

The iteration stated in equation (4.30) will be used until the solutions of two sequential steps are close enough to each other.

A sufficient initial guess is needed. The initial guess used will be the steady state result of the time dependent Runga Kutta method.

For the time independent numerical method again a Python code will be constructed. This Python code can be found via appendix A. The structure for the method used in this part is visualized in figure 9.
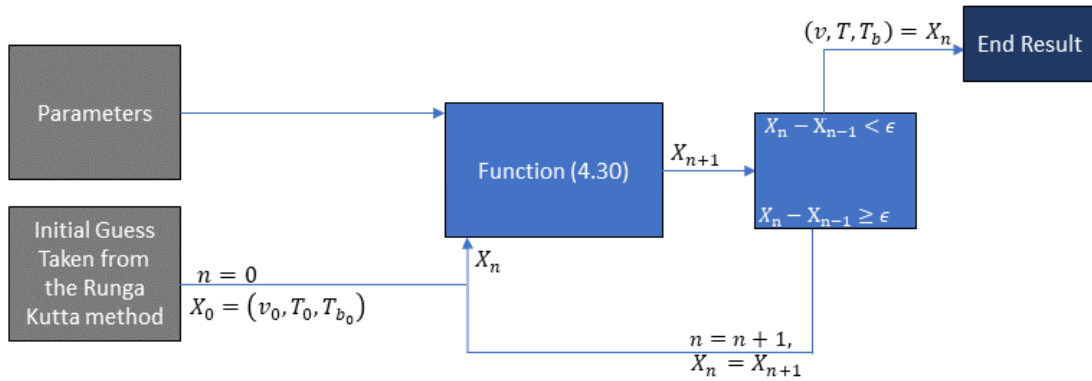


Figure 9: *Method of solving the time independent numerical system.*

## 4.5 Analytical method

The form of the solution for the analytical method is already known, since this is derived in subsection 4.2.4 and subsection 4.3.2. This solution is described in equation (4.17) and equation (4.27). These equations are pretty hard to work out on paper since the friction in equation (4.27) and the constants $A_n$, $B_n$ & $\alpha_n$ are all dependent on the velocity. So an iterative method will be used to determine the velocity.

Since it is needed to determine an integral numerical, a discretization is needed to determine this integral, the same discretization as used in the numerical method is used here. For this method also an initial guess is again needed for the temperature of the fluid, for this the solution of the numerical method will be used.

First the integral in equation (4.27) should be determined with a numerical integrator. For this a simple integration is used, described in equation (4.31),

$$\int_0^L T(l)dl = \sum_{n=0}^{N} \left( \Delta L_n \, T_n \right), \tag{4.31}$$

with $T$ the temperature as a function of $l$, $N$ the number of segments, $\Delta L_n$ the length of segment $n$ and $T_n$ the temperature in segment n.

After the numerical integrator is used to determine the velocity, a new temperature will be calculated with the help of equation (4.17). After this, the next iteration begins with determining a new velocity. This iteration will last until two sequential velocities will be close enough to each other. With the last velocity from these iterations, the final temperature profile will be determined.

For this part, the iterative method, again a Python code will be constructed. This Python code can be found via appendix A. The structure of the used code is visible in figure 10
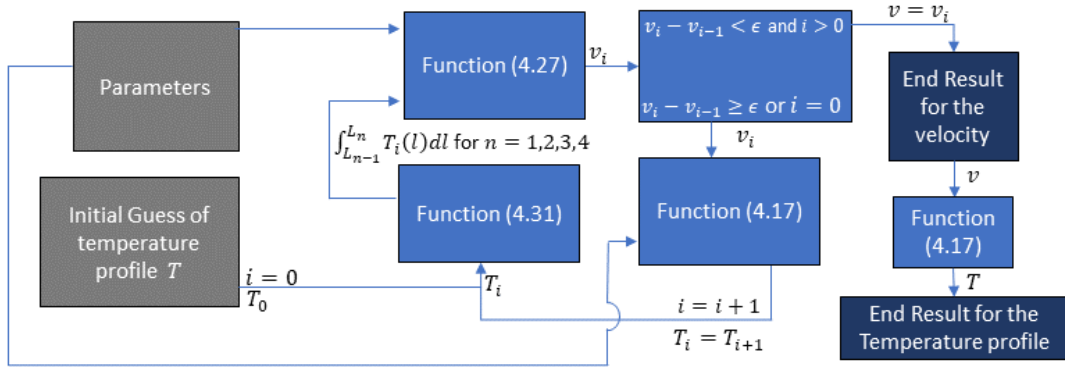


Figure 10: *Method of solving the time independent analytical system.*

# 5 Results

In this section, the results are shown and discussed. First, the parameters are stated. After that, the results of the three methods are discussed. Finally, the results for the influence of the measures within the system and the results of variation of some parameters are shown and discussed.

## 5.1 Parameters

The parameters described in table 1 where used to determine the results.

| Description | symbol | value | unit | reference |
|---|---|---|---|---|
| Gravitational constant | $g$ | 9.81 | m/s$^2$ | [3] |
| Number of Avogadro | $N_a$ | $6.022045 \cdot 10^{-23}$ | mol$^{-1}$ | [3] |
| Angle of horizontal pipes in system | $\phi$ | $5^o$ | - | - |
| Number of segments used in discretisation | $N$ | 40 | - | - |
| Gamma heating generation | $u$ | 300 | $\frac{\text{W}}{\text{kg}}$ | [19] |
| Neutron flux in the HOR in front of the reactor | $\Phi$ | $3.5 \cdot 10^{16}$ | m$^{-2}$ s$^{-1}$ | [19] |
| Average temperature of surrounding water | $T_C$ | 40 | $^o$C | [19] |
| specific heat capacity of water at $40^o$C | $C_{p_{water}}$ | 4181.6 | J/(kg K) | [3] |
| Density of water at $40^o$C | $\rho_{water}$ | 992.25 | kg/m$^3$ | [3] |
| Dynamic viscosity of water at $40^o$C | $\mu_{water}$ | $0.653 \cdot 10^{-3}$ | Pa s | [3] |
| Thermal conductivity of water at $40^o$C | $\lambda_{water}$ | 0.627 | W/ (m K) | [3] |
| Solubility of a Sodium molybdate | $S$ | 84 | g/100ml | [13] |
| Molar mass of a Sodium molybdate | $M_{MoNa_2O_4}$ | 207.8646 | g/mol | [13] |
| Neutron cross section of Mo98 | $\sigma_{Mo98}$ | $130 \cdot 10^{-3}$ | b*** | [11] |
| Molar mass of Mo99 | $M_{Mo99}$ | 98.9077 | g/mol | [14] |
| Specific heat capacity of NaCl solution | $C_p$ | 3327 | J/(kg K) | [9] |
| Reference density of NaCl solution | $\rho_0$ | 1147 | kg/m$^3$ | [9] |
| Thermal conductivity of NaCl solution | $\lambda$ | 0.530 | W/(m K) | [9] |
| Dynamic viscosity of NaCl solution | $\mu$ | $f(\mu_{water}, T)$ ** | Pa s | [10] |
| Molar mass of NaCl | $M_{NaCl}$ | 58.443 | g/mol | [10] |
| Solubility of NaCl | $S_{NaCl}$ | $36 \cdot 10^{-3}/1000$ | mol/kg | [15] |
| Thermal expansion coefficient | $\beta$ | $4.57 \cdot 10^{-4}$ * | K$^{-1}$ | [3] |
| Specific heat capacity of zircolay | $C_{p_{wall}}$ | 285 | J/(kg K) | [19] |
| Density of zircoly | $\rho_{wall}$ | $6.55 \cdot 10^3$ | kg/m$^3$ | [19] |
| Thermal conductivity of zircolay | $\lambda_{wall}$ | 21.5 | W/(m K) | [19] |
| Effective roughness of zircolay | $\epsilon$ | $1.5 \cdot 10^{-6}$ | m | [19] |

Table 1: *Table of parameters used in this system.*
*this value is taken for water since this value for a solution of sodium chloride was not found.*
**this function is further described in the text below.*
*** barn=$10^{-28}m^2$
.

Note that for the dynamic viscosity of the sodium chloride solution a function is taken dependent on the dynamic velocity of water and the temperature. From Aleksandrov et al. [10] an expression is given for the dynamic viscosity of the salt which is, $\mu_{\text{NaCl Solution}} = \mu_{rel}(T) \cdot \mu_{water}(T)$. The term $\mu_{rel}(T)$ stands for the relative dynamic viscosity, which is a dimensionless ratio between the dynamic viscosity of water and the dynamic viscosity of the salt solution. Also in the results of Aleksandrov et al. [10] it is seen that the relative dynamic viscosity $\mu_{rel}$ is strongly dependent on the temperature and could not be taken as a constant. Thus, for this an approximation is made

from the results obtained by Aleksandrov et al. [10], this approximation is shown in equation (5.1),

$$
\begin{aligned}
A &= 0.008 - \frac{0.005}{60}(T - 293.15), \\
B &= 0.06 + \frac{0.06}{60}(T - 293.15), \\
\mu_{rel} &= 1 + A \cdot m^{\frac{1}{2}} + B \cdot m,
\end{aligned}
\tag{5.1}
$$

with $m = M_{NaCl}/S_{NaCl}$ the molality of the solution in [(mol NaCl)/(kg of water)], in this $M_{NaCl}$ stands for the molar mass of sodium chloride and $S_{NaCl}$ stands for the solubility of sodium chloride in water.

## 5.2 Results of the different methods

To obtain the results of the methods the following proportions are taken in the system, the point in the tube where the thickness changes is at the half of the total length, so in the top right corner of the system. In the first half, the thickness of the wall of the tube is taken to be $\delta R = 7$ mm and in the second half, this is a thickness of $\delta R = 1$ mm. For the radius inside the tube the following value is taken, $R = 3$ mm. These measures can also be seen in figure 11a. For the results there will be referenced to different regions of the loop, these regions are shown in figure 11b. With region 1 the first quarter of the tube, the horizontal heating part. Region 2 is the second quarter of the tube, the vertical heating part. Next is region 3, which is the third quarter of the tube, the horizontal cooling part. Lastly is region 4, which is the fourth quarter of the tube, the vertical cooling part.
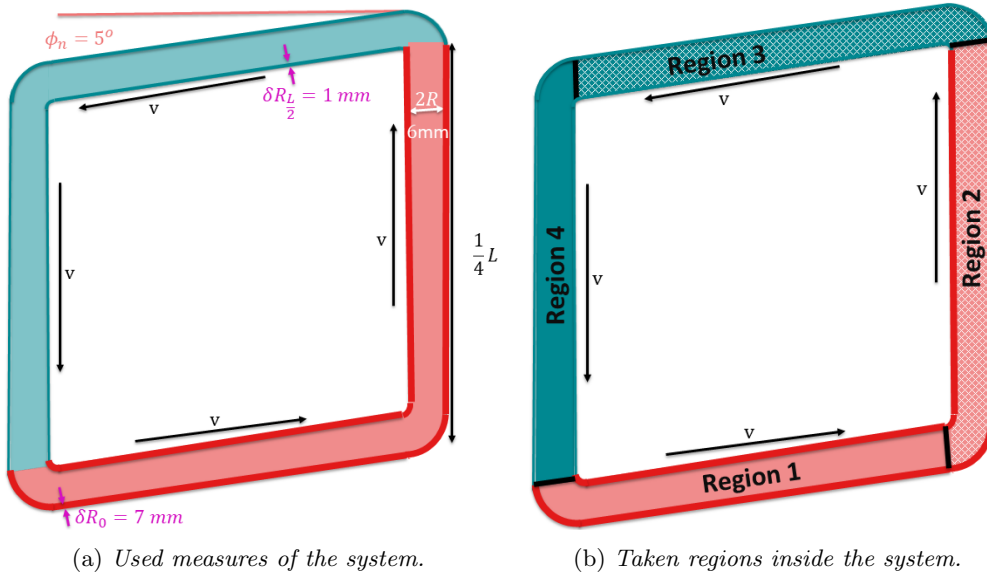
(a) *Used measures of the system.*

(b) *Taken regions inside the system.*

Figure 11: *Visualisation of the system.*

First, the results of the Runga Kutta method are discussed, so it is checked if the system goes towards a steady state. Secondly, provided that a steady state occurs, there is looked at the results of the Newton Raphson method and this is compared to the steady state result of the Runga Kutta method. Lastly, the analytical method is discussed and compared with the result of the numerical method. In the appendix also the stability of the methods and energy conservation of the results are looked into.

### 5.2.1 Runga Kutta method

Like just mentioned, first the results of the Runga Kutta method are evaluated. For the initial condition, a velocity of $v_0 = 10^{-25}\frac{m}{s}$ is used and the initial temperature of both the fluid and the wall are both taken at the room temperature $T_0 = 293.15$ K. In figure 12 the result of the velocity is visualized.
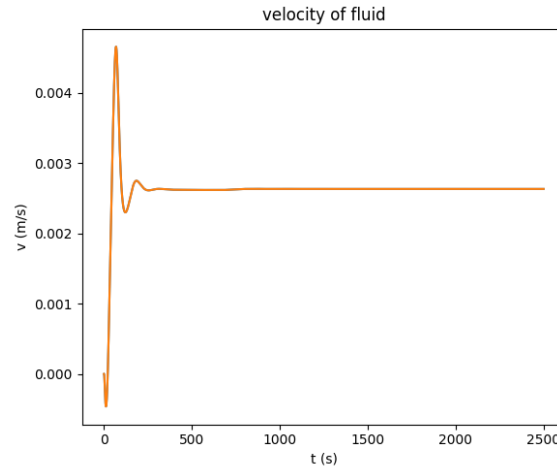


Figure 12: *The velocity of the fluid $[\frac{m}{s}]$ plotted against time [s] of the Runga Kutta method.*

In figure 13 the results of the temperatures of the fluid and the temperatures of the wall are visualized as mean temperatures over four different regions. These regions are visualized in figure 11b.
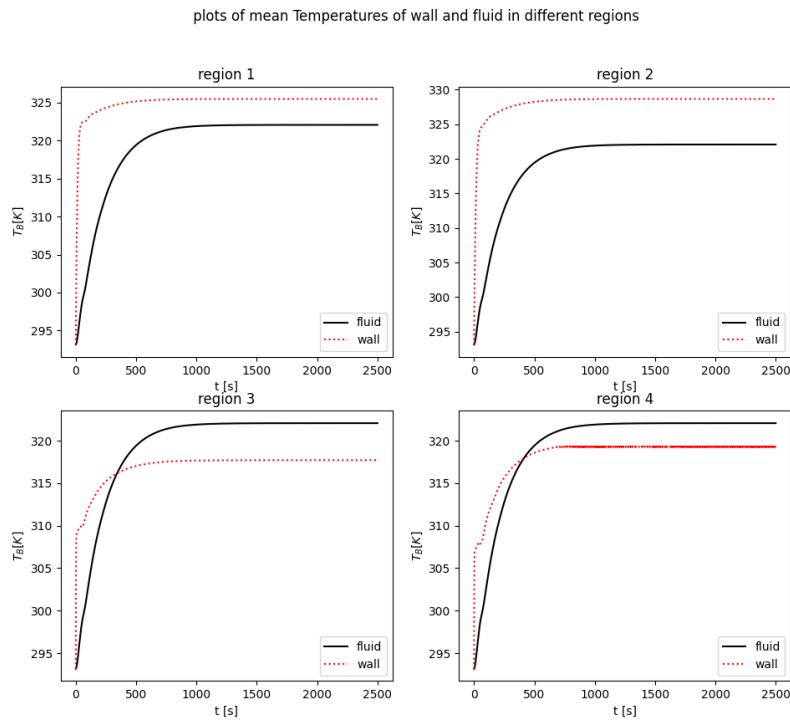


Figure 13: *Mean temperature of the fluid and the wall [K] in a certain region of the tube, with the tube divided into 4 regions. These regions are visible in figure 11b.*

In figures 12 and 13 can be seen in the plots that the system goes towards a steady state with a velocity of $2.6\frac{mm}{s}$. In figure 12 can be seen that in the beginning, the velocity is first negative and soon becomes positive. This effect can occur since in regions 3 and 4 the wall is thinner than in regions 1 and 2 and the initial temperature is taken below the temperature of the surrounding water. This means that the system, in the beginning, will not only be heated by gamma heating but also by the surrounding water. Since the second part of the tube has a thinner wall this part will sooner be heated by the water, which results in a lower density in this part. This causes the fluid to flow in the negative direction until gamma heating is the dominating source of heating.

When looking at figure 13 it can be seen that in the beginning, the values do not go smoothly to the steady state, there is a small deviation in the beginning. This deviation is due to the velocity which is not steady yet and shows steep changes with respect to time at the beginning of the time period. These changes in the velocity causes the temperature of the wall to fluctuate in the beginning.

Note that the temperature of the wall in region 1 and region 2 is higher than the temperature of the fluid, this results in heating of the fluid in these regions. In region 3 and region 4 can be seen that the temperature of the fluid is higher than the temperature of the wall, which results in cooling of the fluid.

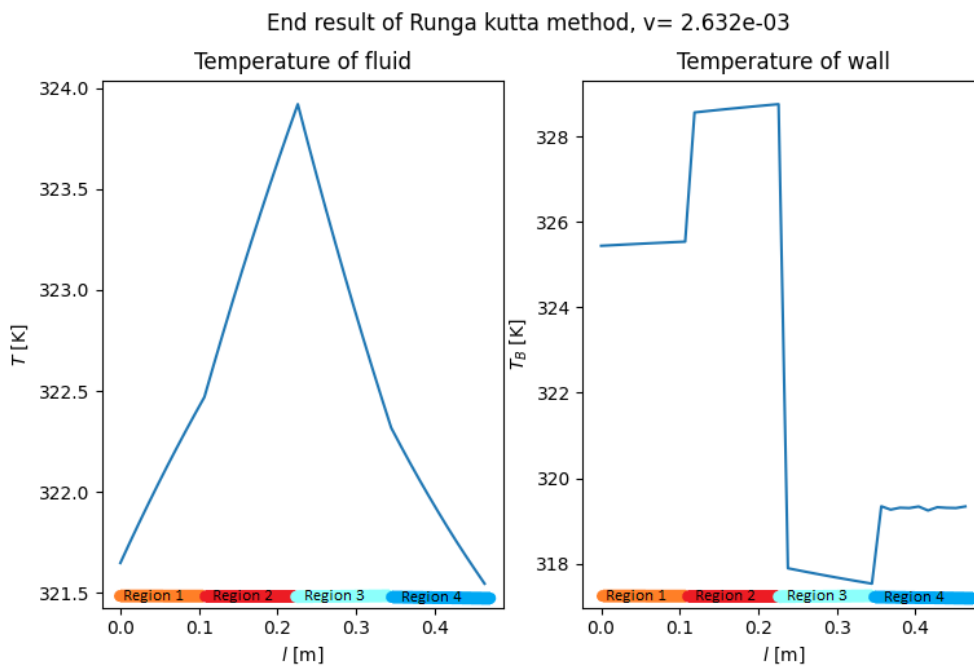The steady state obtained by this method is shown in figure 14.



Figure 14: *The steady state result of the Runga Kutta method is shown in this figure. In the left plot the temperature profile of the fluid inside the tube [K] and in the right plot the temperature profile of the wall [K].*

The temperature profile visible in figure 14 is indeed what was expected. Since the first half of the tube will heat the fluid and the second part of the tube is designed to cool the fluid, since this has a thinner thickness of the wall. Additionally it is seen that in the first region the heating will be less than in the second region. This makes sense since the first region is horizontal and the second region is vertical. The wall of the vertical part loses less energy to the surrounding water, because of natural convection of the water, so the wall of the vertical part will lose more energy to the fluid inside the tube in comparison to the horizontal part. This results in more heating of the fluid in the vertical part than in the horizontal part. This difference between the vertical and horizontal part can also be seen in the cooling part of the system. The third region of the tube, which is the

horizontal tube, will cool the fluid more than the fourth region of the tube, which is the vertical tube. This is also due to the natural convection in the surrounding water. So the horizontal part will cool better than the vertical part of the loop.

In appendix D also a variation of the initial conditions is made, to make sure the system will go to this steady state for other initial conditions, which indeed happens. Initial conditions used, range for the temperature from $10^oC$ to $80^oC$ and for the velocity from $0.0001\frac{m}{s}$ to $0.2\frac{m}{s}$.

### 5.2.2 Newton Raphson method

Since the Runga Kutta method goes to a steady state, there will now be looked at the Newton Raphson method. The result of this method for the velocity is the following value $v = 2.6\frac{mm}{s}$ and for the temperature the values are shown in figure 15. In figure 15 also the steady state result of the Runga Kutta method is present, so the results of the two methods can be compared.
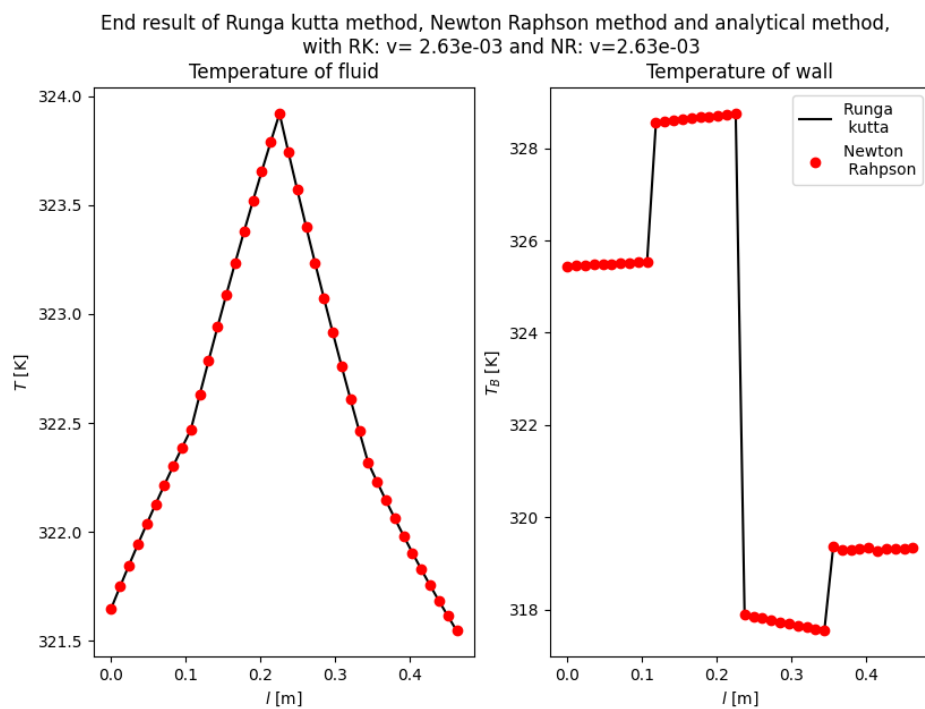


Figure 15: *Result of the temperature from the Newton Raphson method, the red points, and the steady state result of the Runga Kutta method, the solid line, with in the left plot the temperature profile of the fluid inside the tube [K] and in the right plot the temperature profile of the wall [K].*

It is seen in figure 15 that the two results of the temperature agree. Both methods give the same velocity, $v = 2.6\frac{mm}{s}$.

### 5.2.3 Analytical method

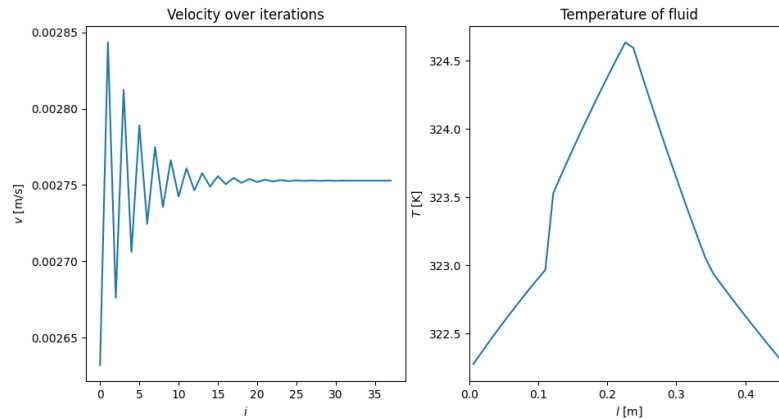Lastly, the results of the analytical method will be discussed. The results of this method are shown in figure 16.



Figure 16: *Result of the analytical method,*
*with in the left plot the velocity of the fluid $[\frac{m}{s}]$ against the iterations used to obtain this velocity*
*and in the right plot the temperature profile of the fluid [K].*

It is seen that the velocity converges to a value of $v = 2.8\frac{\text{mm}}{\text{s}}$, which is a slightly higher value than the values obtained in the previous two methods, $v = 2.6\frac{\text{mm}}{\text{s}}$. The values of the temperature in figure 16 also seems to be slightly higher. A plot is made with both the numerical result and the analytical result, which is seen in figure 17.
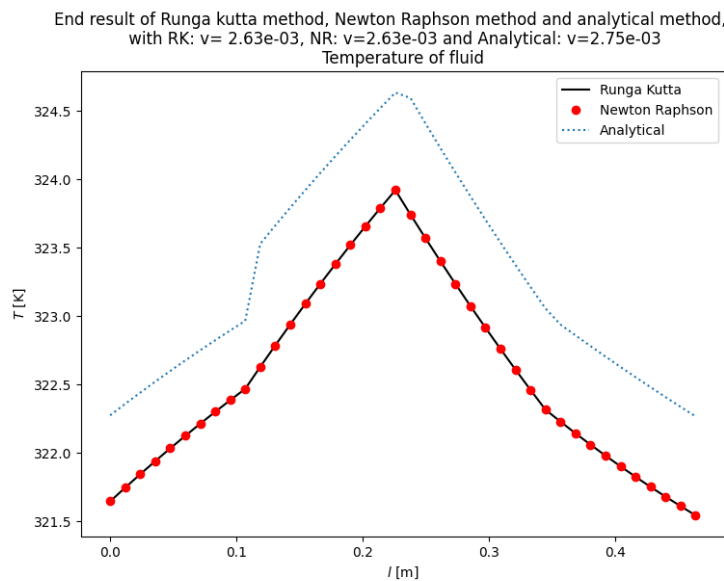


Figure 17: *Result of the temperature profile [K] of the analytical method, the dotted line, the Newton Raphson method, the red points and the Runga Kutta method, the solid line.*

In figure 17, can indeed be seen that the temperature of the result of the analytical method is slightly higher than the temperate of the results of the numerical methods. Differences in the results can be a result of simplifications made for the analytical method. Despite these simplifications, the differences in the results of the numerical methods and the analytical method are remarkably small.

## 5.3 Analysing the influence of the measures in the system

To see for which measures this system has a safe temperature and a velocity of the fluid will occur, the measures are varied. For the results in this section, the time independent numerical method is used. Since this method does not contain simplification and the time for finding a steady state solution is smaller with this method than with the time dependent numerical method.
Firstly, measures of the thicknesses of the wall are varied, then the measure of the radius of the tubes is varied and lastly the part of the system which is heated and which is cooled is varied.

### 5.3.1 Varying the thickness of the wall

First, the thickness of the wall is varied. The thickness of the wall of the cooling part of the loop is varied from $\delta R = 0.5$ mm to $\delta R = 40$ mm. The thickness of the wall of the heating part of the loop is varied from $\delta R = 1$ mm to $\delta R = 40$ mm. The resulting velocities and highest temperatures in the loop are plotted, which is visible in figure 18.



(a) *Velocity of fluid $[\frac{m}{s}]$.*        (b) *Highest temperature of fluid inside the loop [K].*
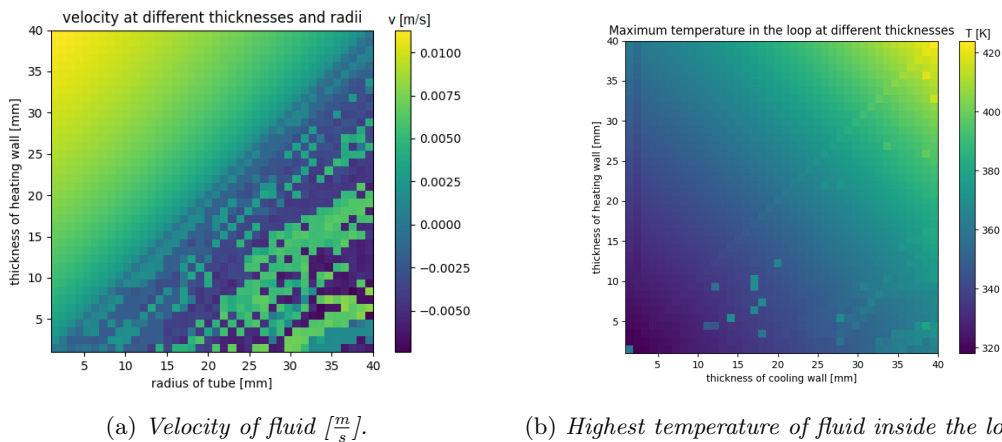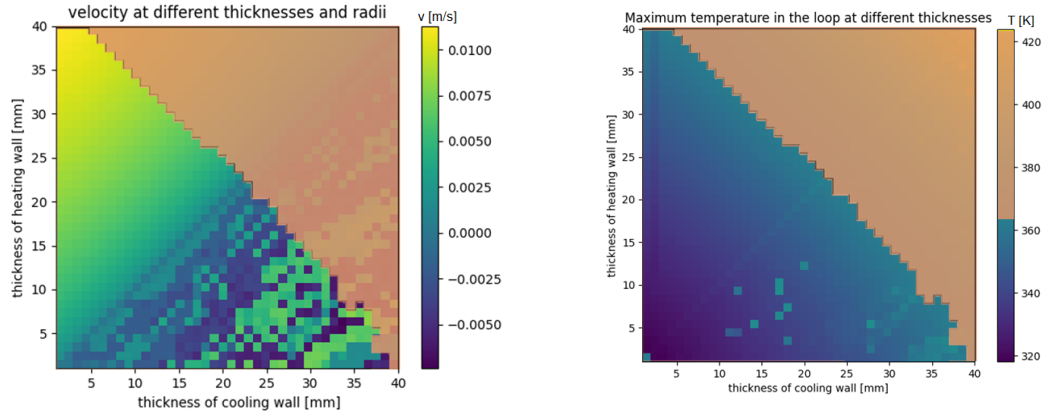
Figure 18: *The velocity and the highest temperature of fluid inside the loop at different thicknesses of the cooling and heating wall.*

In figure 18a it is seen that a higher thickness of the heating wall will most of the time result in a higher velocity. This is not always the case, since a higher thickness of the heating wall can also result in a higher overall heat of the fluid instead of a higher heat difference within the loop. A thickness of the heating wall which is around the same as the thickness of the cooling wall will result in a velocity around zero, which is expected since both cooling en heating parts will have around the same heat exchange for which the natural convection will not occur inside the loop.

In figure 18a can be seen that at thicknesses of the wall where the wall of the cooling part is thicker than the wall of the heating part, the system has a complex patron for the velocity, different from the profile for the velocity in the top left of the plot. The reason for this complex patron is that the system is build to be heated in the first part of the tube and cooled in the second part of the tube. When this is turned around, the heating is not optimal since this then will happen at the top of the loop instead of the bottom, also the angle in the loop can affect the current. So for some values of the thickness of the wall, a negative velocity is obtained, this is only if the thickness of the cooling wall is big enough and the thickness of the heating wall is small enough, but when the thickness of the heating wall is too large relative to the thickness of the cooling wall the geometry of the loop will force the velocity to be positive. In figure 18a in the bottom right, an irregular pattern is observed, a reason for this can be that the solution can be very dependent on the initial conditions.

When taking a look at figure 18b it can be seen that the temperatures inside the loop can be very high, which is of course not always desirable when looking at safety. For safety reasons, the temperature of the loop is desired to stay below 90°C. Thus, the allowed region of the thicknesses of the wall is shown in figure (19).
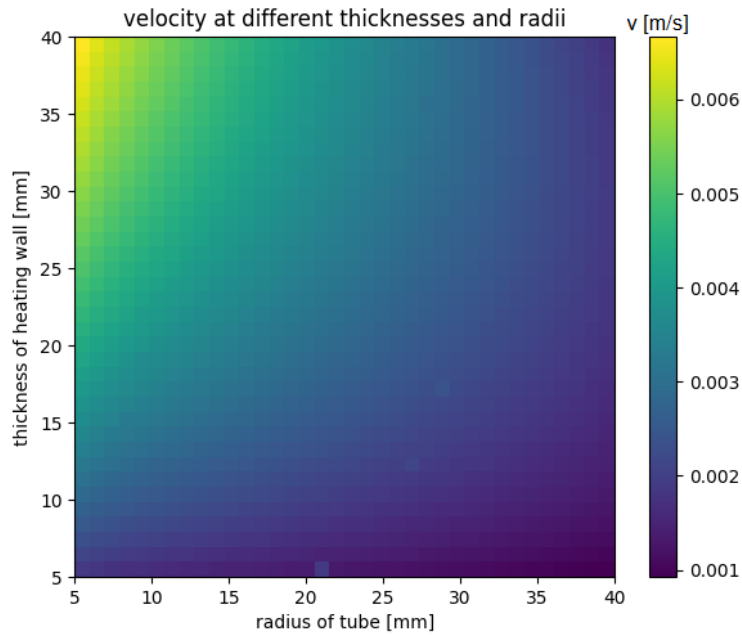


(a) *Velocity of fluid $[\frac{m}{s}]$.*

(b) *Highest temperature of fluid inside the loop [K].*

Figure 19: *The velocity and the highest temperature of the fluid inside the loop at different thicknesses of the cooling and heating wall. The orange part is the region where the maximum temperature of the loop is above 90° C.*

The thickness of the cooling wall from now on is taken to be $\delta R = 1$ mm. The heating wall is varied along with the radius of the tube in the next subsection.

### 5.3.2 Varying the radius of the tube and the thickness of the heating wall

The radius of the tube and the thickness of the heating wall are both varied from 5mm to 40mm. The velocity, the highest temperature in the loop, the length of the loop, the volume of the loop and the reaction rate per second of the loop are all shown in figure 20 and figure 21.
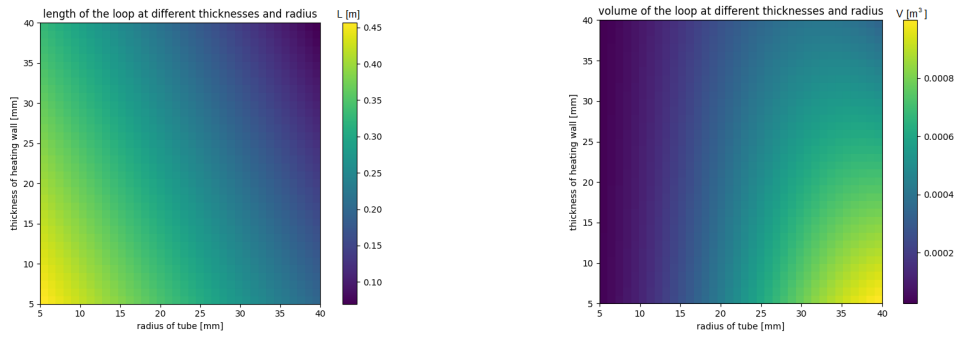


(a) *Velocity of fluid $[\frac{m}{s}]$.*
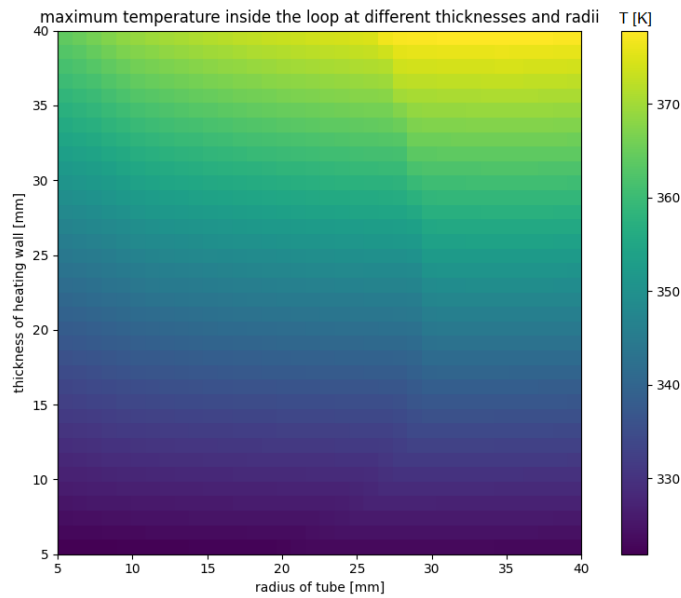


(b) *Highest temperature of fluid inside the loop [K].*

Figure 20: *The velocity and the highest temperature of fluid inside the loop.*
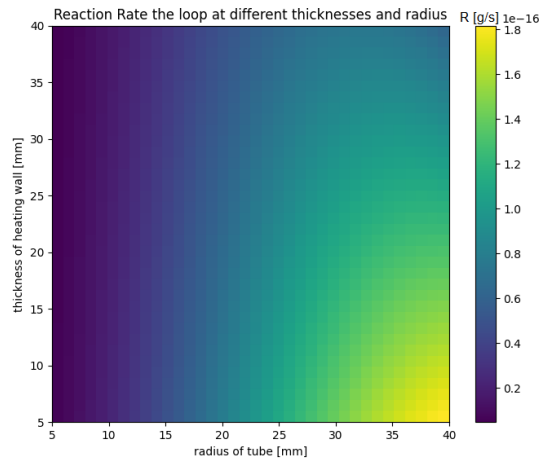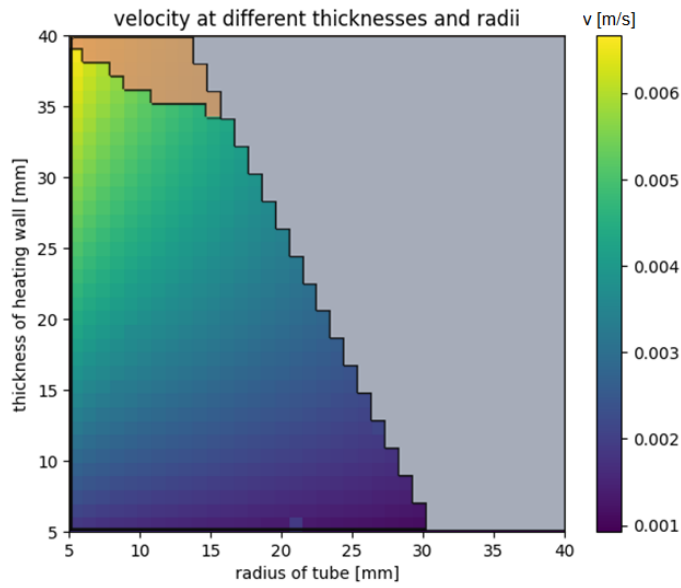
(a) *Length of the loop [m].*



(b) *Volume of fluid inside the loop [m³].*



(c) *Reaction rate of molybdenum[99] per second inside the loop*
$[\frac{g}{s}]$.

Figure 21: *The length of the loop, the volume of the fluid inside the loop and the reaction rate inside the loop at different radii of the tube and thicknesses of the heating wall.*

- It can be seen in figure 21c that the reaction rate is higher as the volume of the fluid is higher, this makes sense since more fluid means more molybdenum[98] which can create molybdenum[99].

- It is visible in figure 20a that the velocity of the fluid is again most of the time higher for a thicker wall in the heating part.

- Thirdly, in figure 20a can be seen that the velocity fastly decays when the radius of the tube gets bigger. The velocity decays drastically for a higher radius since it is harder to heat a bigger volume, $V_{\text{fluid}}$, which is dependent on the radius squared, $R^2$.

To have a reaction rate as high as possible, a high radius of the tube is needed.

The temperature can be seen in figure 20b to again exceeds the desired temperatures at some thicknesses of the heating wall and radii of the tube. This is again added in the plots, visible in figure 22 and figure 23. But one restriction is not yet included. A quarter of the length of the tube can never be smaller than the thickness of the heating wall, the thickness of the cooling wall and two times the radius of the tube summed, this can easily be seen in figure 3a in section 2 Design. Thus with this restriction and the maximum temperature applied figure 22 and figure 23 is shown with the possible values.

(a) *Velocity of fluid $[\frac{m}{s}]$.*
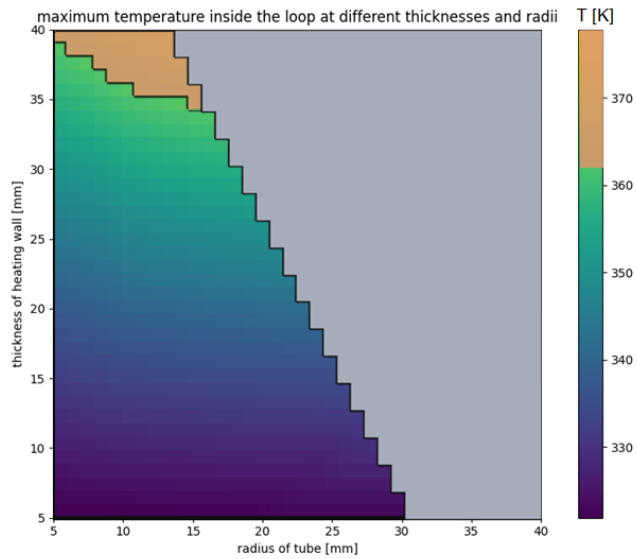


(b) *Highest temperature of fluid inside the loop [K].*

Figure 22: *The velocity and the highest temperature of the fluid inside the loop, the length of the loop, the volume of the fluid inside the loop and the reaction rate inside the loop at different radii of the tube and thicknesses of the wall of the heating part. The gray part is the region that is not possible due to the restriction. The orange part is the region where the maximum temperature of the loop is above $90^{o}C$.*
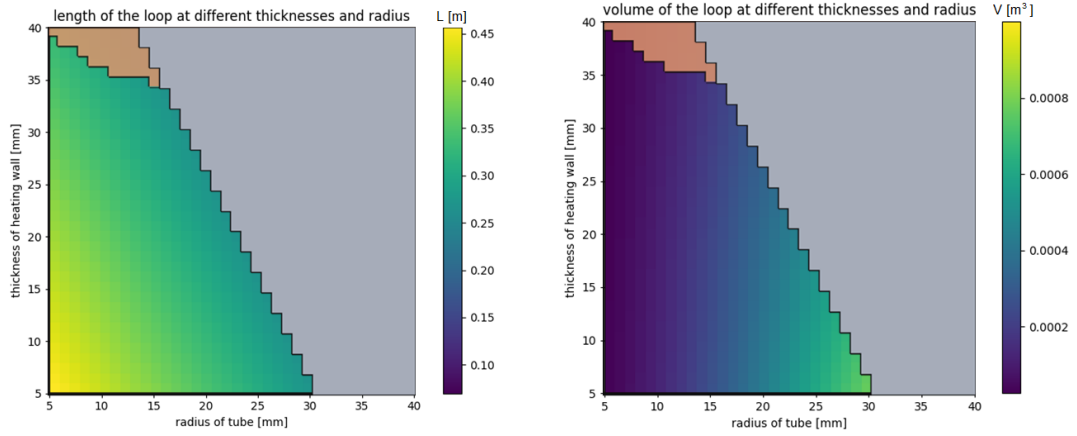
(a) *Length of the loop [m].*

(b) *Volume of fluid inside the loop $[m^3]$.*
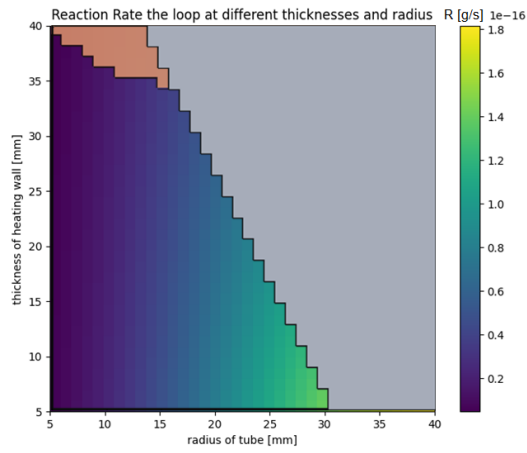


(c) *Reaction rate of molybdenum$^{99}$ inside the loop* $\left[\frac{g}{s}\right]$.

Figure 23: *The volume of the fluid inside the loop and the reaction rate inside the loop at different radii of the tube and thicknesses of the wall of the heating part. The orange part is the region that is not possible due to the restriction.*

The following value for the radius of the tube is taken from now on, $R = 20$mm. The value for the thickness of the heating wall is again varied in the next section along with varying the part of the system which will heat the fluid.

### 5.3.3 Varying the heating and cooling part

In this subsection, the part of the system which heats the fluid and the part of the system which cools the fluid is varied. In figure 24 it can be seen in the right vertical region that the thickness of the wall will be changed within this region. The location where this change occurs will be varied, so the parameter *part* will be varied.
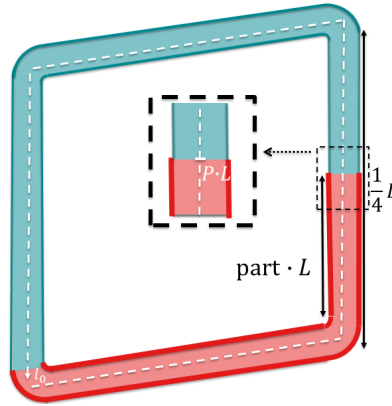


Figure 24: *Visualisation of the setup.*

This is done by varying *part* from 0 to 0.25. This can also be written as at which spatial coordinate $l$, the thickness of the wall changes, $l = P \cdot L$. The origin of this spatial coordinate, $l$, is located in the left bottom corner of the loop. This can also be seen in figure 24. Thus, $P$ in the location at which this thickness is changed, $l = P \cdot L$, will be varied. In this case, this will be varied from $P = 0.25$ to $P = 0.5$. Along with this variation, the thickness of the wall of the heating part will also be varied, from $\delta R = 10$mm to $\delta R = 30$mm. The values obtained by this variation are plotted and shown in figure 25.



(a) *Velocity of fluid $[\frac{m}{s}]$.*

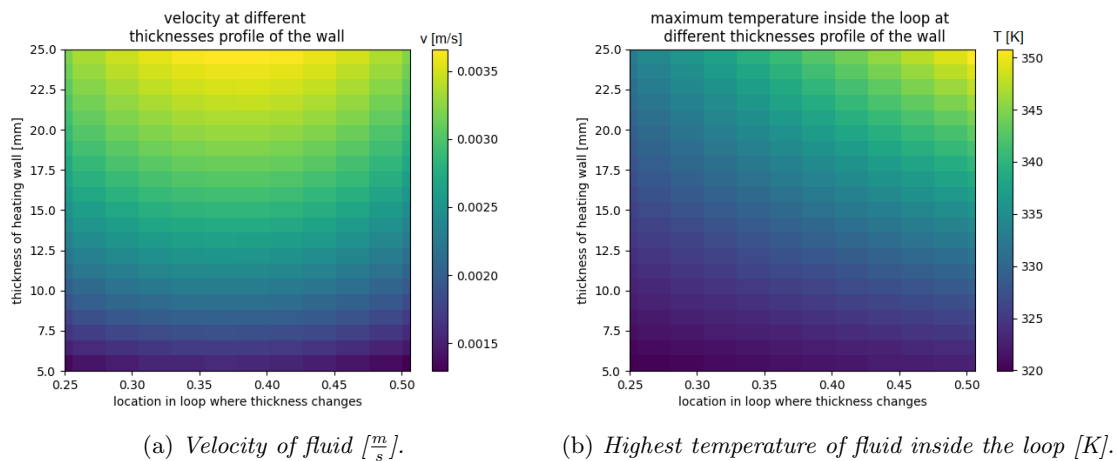(b) *Highest temperature of fluid inside the loop [K].*

Figure 25: *The velocity and the highest temperature of fluid inside the loop are shown for different parts of the loop heated and different thicknesses of the wall of the heating part.*

In figure 25b it is visible that the temperature does not exceed the safety limit. In figure 25a it seems the velocity of the fluid is highest when the location of the end of part 1 of the loop is around $0.4L$. The reason it is lower in the other regions is that this is the optimal heating and cooling proportion in which the temperature differences in the system will be highest, which causes a higher velocity.

The plot seems to be divided into 10 different regions when looking in the direction of the x-axis, this is explained by the segments token earlier, since in the second region, the first vertical part,

of the loop only 10 segments are present.

The velocity is highest when the location of the end of part 1 of the loop is $0.4L$ and the thickness of the heating wall is $\delta R = 25$mm. At this point, the velocity is $v = 3.7\frac{\text{mm}}{\text{s}}$. However, as seen in the last subsection the reaction rate is lower for a higher thickness of the heating wall.

The following values are taken for the results in the next subsection: thickness of the heating wall $\delta R = 15$mm, thickness of the cooling wall $\delta R = 1$mm, radius of the tube $R = 20$mm and the location of end of part 1 of the loop is taken at $0.4L$. For this values the following results are obtained: the velocity $v = 2.8\frac{\text{mm}}{\text{s}}$ , the reaction rate $R = 7.1 \cdot 10^{-17}\frac{\text{g}}{\text{s}}$ and the temperature profile shown in figure 26.
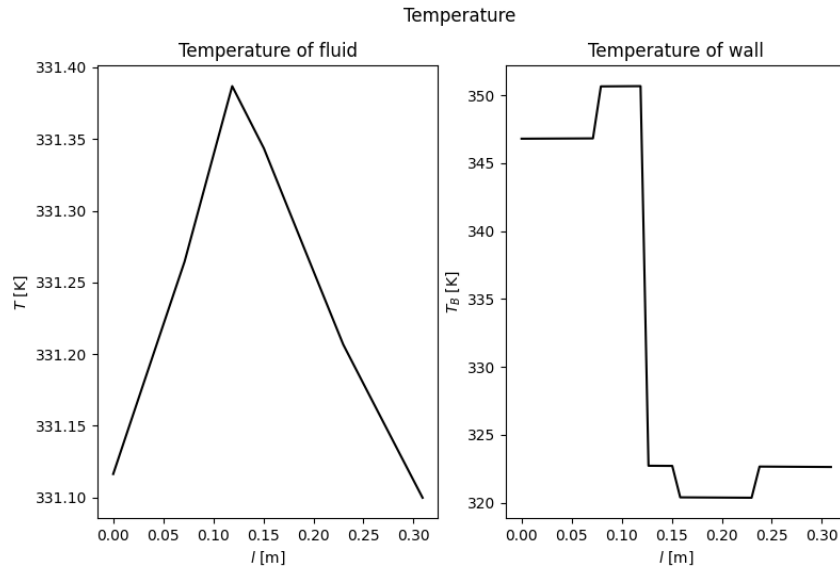


Figure 26: *Temperature profile of the system. With in the left plot the temperature profile of the fluid [K] and in the right plot the temperature profile of the wall [K].*

## 5.4 Variation of fluid properties

In this section, the properties of the fluid will be varied. This will be done by multiplying these parameters with a constant $K_{parameter}$. The properties used for the fluid will be varied since the exact values of these parameters were not obtained. These parameters are the specific heat capacity $C_p$, the density $\rho_0$, the thermal conductivity $\lambda$, the dynamic viscosity $\mu$ and the thermal expansion coefficient $\beta$.

### 5.4.1 Variation of the specific heat capacity

The specific heat capacity will be varied with the constant $K_{C_p}$ between $K_{C_p} = 0.3$ and $K_{C_p} = 3$. The results of the velocity and the temperature profile of this parameter variation are seen in figure 27.



(a) *Velocity of fluid $\left[\frac{m}{s}\right]$.*  (b) *Temperature profile of fluid [K]*
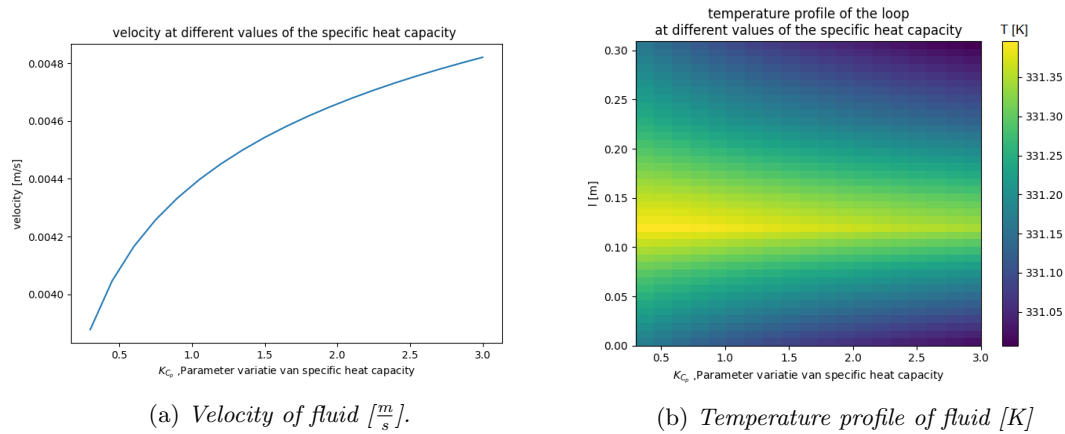
Figure 27: *Variation of the parameter specific heat capacity from $K_{C_p} = 0.3$ to $K_{C_p} = 3$.*

As seen in figure 27a The change of the specific heat capacity does change the velocity, but within this change the velocity stays stable. The same is true for the temperature profile as seen in figure 27b, the change of the temperature is relatively small. This is desirable since the specific heat capacity of a sodium chloride solution is used in this model. This means that even if the heat capacity of the molybdenum salt solution that will be used will fall within the variation with the constant $K_{C_p}$ between $K_{C_p} = 0.3$ and $K_{C_p} = 3$ the model still produces a stable result, which has not changed to much from the result obtained in this thesis.

### 5.4.2 Variation of the density

The density will be varied with the constant $K_{\rho_0}$ between $K_{\rho_0} = 0.3$ and $K_{\rho_0} = 3$. The results of the velocity and the temperature profile of this parameter variation are seen in figure 28.
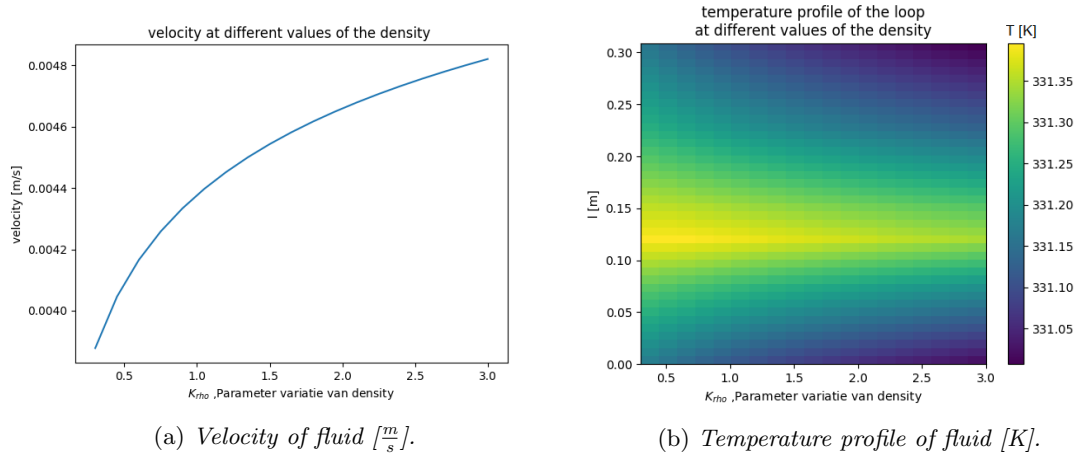


(a) *Velocity of fluid $[\frac{m}{s}]$.*

(b) *Temperature profile of fluid [K].*

Figure 28: *Variation of the parameter density from $K_{\rho_0} = 0.3$ to $K_{rho_0} = 3$.*

As seen in figure 28a and 28b the change of the density does change the velocity and the temperature profile at an equal range as the variation of the specific heat capacity did. This makes sense since the system is equally dependent on the specific heat capacity as on the density, this can be seen in the derivation earlier in the section 4 Methods. Thus the same is true for the variation of the density as was for variation of the heat capacity coefficient. This again is desirable, for the same reasons mentioned in the last subsection.

### 5.4.3 Variation of the thermal conductivity

The thermal conductivity will be varied with the constant $K_\lambda$ between $K_\lambda = 0.3$ and $K_\lambda = 3$. The results of the velocity and the temperature profile of this parameter variation are seen in figure 29.



(a) *Velocity of fluid $[\frac{m}{s}]$.*

(b) *Temperature profile of fluid [K].*
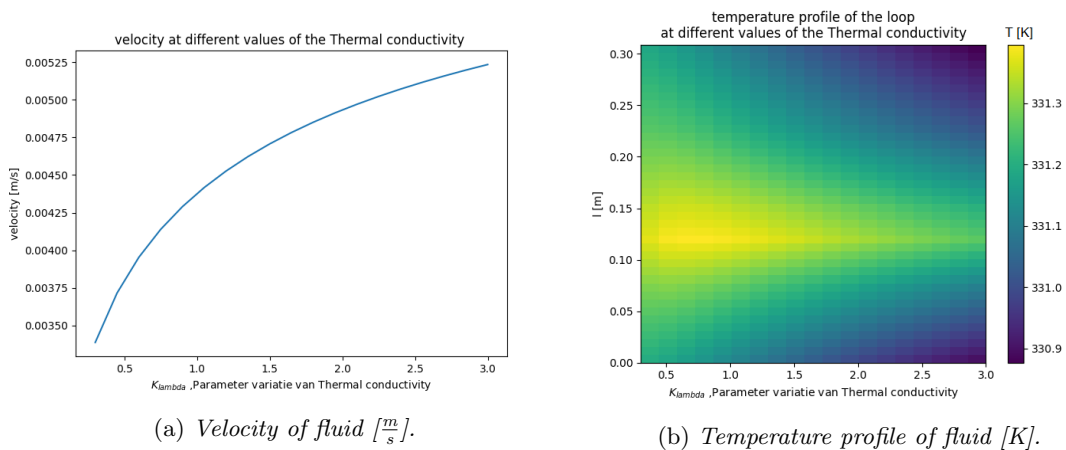
Figure 29: *Variation of the parameter thermal conductivity from $K_\lambda = 0.3$ to $K_\lambda = 3$.*

As seen in figure 29a the change of the thermal conductivity does change the velocity, this change is a little bit more than the previous two variations, but within this change the velocity still stays stable and desirable. Also for the temperature profile, this variation changes slightly more than the last two variations as seen in figure 27b, the change of the temperature is however still relatively

small. So as long as these changes stay within a wanted range for the variable and stay stable, this is still desirable. Also for this parameter, the thermal conductivity, the same reasoning why this is desirable applies as the last parameters discussed

### 5.4.4 Variation of the dynamic viscosity

The dynamic viscosity will be varied with the constant $K_\mu$ between $K_\mu = 0.3$ and $K_\mu = 3$. The results of the velocity and the temperature profile of this parameter variation are seen in figure 30.



(a) *Velocity of fluid [$\frac{m}{s}$].*



(b) *Temperature profile of fluid [K].*
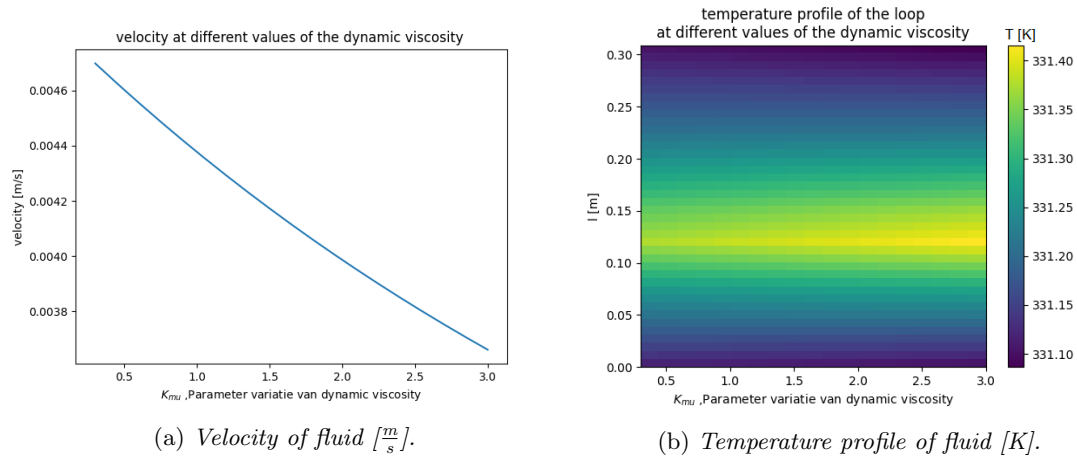
Figure 30: *Variation of the parameter dynamic viscosity from $K_\mu = 0.3$ to $K_\mu = 3$.*

As seen in figure 30a The change of the dynamic viscosity causes a relatively small change in the velocity, which again stays stable. The same is again true for the temperature profile as seen in figure 30b, the change of the temperature is relatively small. Once more this is a desirable outcome for the same reasons mentioned before.

### 5.4.5 Variation of the thermal expansion coefficient

The thermal expansion coefficient will be varied with the constant $K_\beta$ between $K_\beta = 0.3$ and $K_\beta = 3$. The results of the velocity and the temperature profile of this parameter variation are seen in figure 31.
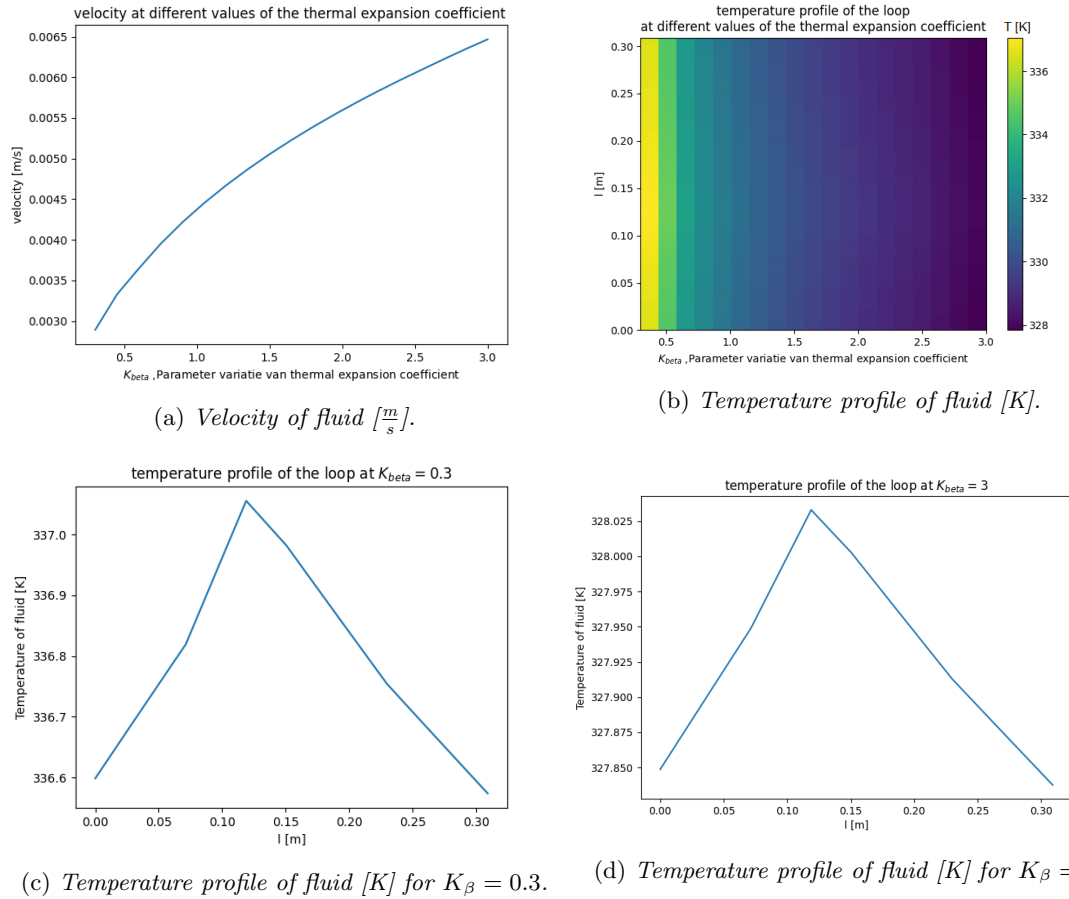


(a) *Velocity of fluid $[\frac{m}{s}]$.*



(b) *Temperature profile of fluid [K].*



(c) *Temperature profile of fluid [K] for $K_\beta = 0.3$.*



(d) *Temperature profile of fluid [K] for $K_\beta = 3$.*

Figure 31: *Variation of the parameter thermal expansion coefficient from $K_\beta = 0.3$ to $K_\beta = 3$.*

As seen in figure 31a the change of the thermal expansion coefficient does change the velocity, here this change is not relatively small anymore, but within this change the velocity stays stable and within the wanted range. The same can be said for the temperature profile as seen in figure 31b, the change of the temperature is relatively large. To have a better look at this change of the temperature two additional plots were made, with the temperature profile for the thermal expansion coefficient variation with the value of the constant at $K_\beta = 0.3$ and at $K_\beta = 3$. These plots can be seen in figure 31c and 31d respectively. In these plots, it can be seen that the form of the temperature profile has not changed, only the value of the temperature at each location has shifted. The temperatures are however still in a desirable region. That both the temperature and the velocity are still in a desirable region is favorable, since for a different thermal expansion coefficient this system is still stable and usable.

### 5.4.6 Variation of multiple properties

To make sure the system still is in a desirable region if all parameters are different, this will be tested for a worst case scenario. For this, the specific heat capacity, the density and the thermal conductivity will all be varied from $K_{C_p} = K_{\rho_0} = K_\lambda = K_\beta = 0.3$ to $K_{C_p} = K_{\rho_0} = K_\lambda = K_\beta = 3$ since all these values cause a rise in the velocity and a decay in the temperature when these parameters rise.

The dynamic viscosity however, causes a decay of the velocity and a rise in the temperature as it rises, so for this the same steps will be taken but backward, so the constant will go from $K_\mu = 3$ to $K_\mu = 0.3$. This means that when this system is calculated for $K_{C_p} = K_{\rho_0} = K_\lambda = K_\beta = 0.3$ the constant of the dynamic viscosity will be $K_\mu = 3$ and when this system is calculated for $K_{C_p} = K_{\rho_0} = K_\lambda = K_\beta = 3$ the constant of the dynamic viscosity will be $K_\mu = 0.3$.

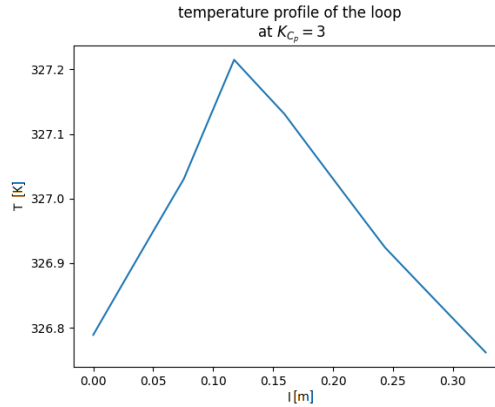For this variation, the results shown in figure 32 are obtained.
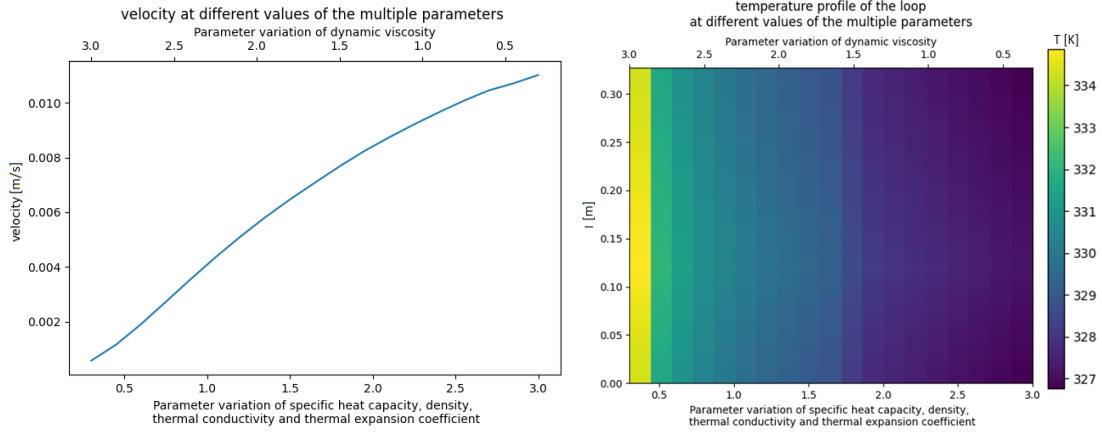


(a) *Velocity of fluid $[\frac{m}{s}]$.*

(b) *Temperature profile of fluid [K].*
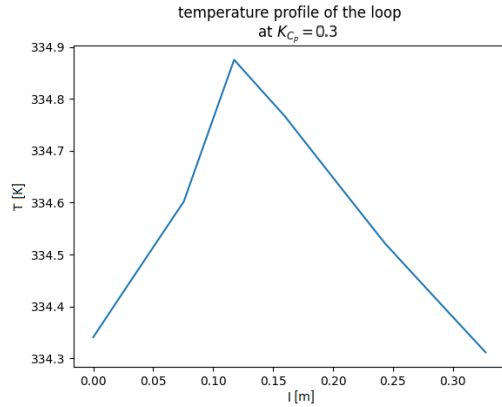
(c) *Temperature profile of fluid [K] for $K_{C_p} = K_{\rho_0} = K_\lambda = K_\beta = 0.3$ and $K_\mu = 3$.*

(d) *Temperature profile of fluid [K] for $K_{C_p} = K_{\rho_0} = K_\lambda = K_\beta = 3$ and $K_\mu = 0.3$.*

Figure 32: *Variation of the parameters specific heat capacity, density, thermal conductivity, thermal expansion coefficient and dynamic viscosity from $K_{C_p} = K_{\rho_0} = K_\lambda = K_\beta = 0.3$ to $K_{C_p} = K_{\rho_0} = K_\lambda = K_\beta = 3$ and $K_\mu = 3$ to $K_\mu = 0.3$.*

From these results, it can be seen that the temperature again only shifts and the temperature profile does not change its form. The current temperatures for these variations are again within a range for which this system is still usable.

A second noticeable change is the change of the velocity over the variation of the parameters. This also changes quite a bit, but also for the velocity the values in this range still provide a suitable system.

The results of the variation of the different fluid properties are combined in table 2.

| Parameter | Range $K_{parameter}$ | Range velocity $\left[\frac{mm}{s}\right]$ | Range maximum temperature $[^{o}C]$ |
|---|---|---|---|
| Specific heat capacity | $\uparrow K_{C_p} = 0.3 \to 3$ | $3.9 \to 4.8 \uparrow$ | $58.3 \to 58.2 \downarrow$ |
| Density | $\uparrow K_{\rho_0} = 0.3 \to 3$ | $3.9 \to 4.8 \uparrow$ | $58.3 \to 58.2 \downarrow$ |
| Thermal conductivity | $\uparrow K_{\lambda} = 0.3 \to 3$ | $3.4 \to 5.2 \uparrow$ | $58.2 \to 58.1 \downarrow$ |
| Dynamic viscosity | $\uparrow K_{\mu} = 0.3 \to 3$ | $4.7 \to 3.7 \downarrow$ | $58.2 \to 58.3 \uparrow$ |
| Thermal expansion coefficient | $\uparrow K_{\beta} = 0.3 \to 3$ | $2.9 \to 6.5 \uparrow$ | $63.9 \to 54.9 \downarrow$ |
| Specific heat capacity Density Thermal conductivity Dynamic viscosity Thermal expansion coefficient | $\uparrow K_{C_p} = 0.3 \to 3$ $\uparrow K_{\rho_0} = 0.3 \to 3$ $\uparrow K_{\lambda} = 0.3 \to 3$ $\downarrow K_{\mu} = 3 \to 0.3$ $\uparrow K_{\beta} = 0.3 \to 3$ | $0.6 \to 9.0 \uparrow$ | $63.6 \to 53.6 \downarrow$ |

Table 2: *Variation of the fluid properties.*

## 5.5 Discussion

The Runga Kutta method showed that the system will go towards a steady state, for further elaboration on this there can be looked at the appendix in which the initial conditions are varied.
The analytical method seems promising since the temperature profile and the velocity are in the same range as the solutions obtained with the numerical method. Despite the simplifications in the analytical method, the values of the temperature are only relatively slightly shifted. Thus, this gives promising results for the analytical method. For even more precise results it can be considered to take more different constants in the derivation of the analytical model, this would be a quite tedious derivation however.

As seen in the last subsections the system is feasible, even if the parameters are changed. The system stays under the temperature of the safety norms, as long as the thicknesses of the wall in the tube do not become too large. The system is quite dependent on the thicknesses of the wall of the tube and the radius of the tube.

The reaction rate of this system will have an order of magnitude of around $7 \cdot 10^{-17} \frac{g}{s}$. This is only of the order of $4 \cdot 10^{-8}$ mg molybdenum$^{99}$ per week. Which is around $4 \cdot 10^{-8}\%$ of the worldwide weekly demand [20]. This is very low, which makes this system not yet an optimal choice for the production of molybdenum$^{99}$.

This thesis has a couple of simplifications and assumptions.

Firstly, the temperature in the wall is taken to be a mean temperature over the following dimensions, the radius of the tube $r$ and the angle of the tube $\theta$. This is of course not the case, there will be a temperature profile inside the wall and since the wall is at certain points in the tube relatively thick, this temperature profile can be a factor for the heat transfer from the wall to the fluid inside the tube and the surrounding water.
The temperature profile will have a certain temperature for the boundary of the wall on side of the fluid, so the inner boundary of the wall. This temperature affects the heat transfer from the fluid to the wall. The temperature profile will most likely have a different temperature at the boundary of the wall on the side of the surrounding water, so the outer boundary of the wall. This temperature again affects the heat transfer from the wall to the surrounding water. In this thesis, these temperatures at the boundaries of the wall are taken equal to each other, as the mean temperature of the wall.
If the temperature profile of the wall is applied in the system, the heat transfer from the fluid to the wall and from the wall to the surrounding water can for example be a lot smaller, which would give higher temperatures inside the system. So the temperature profile of the wall is neglected in this thesis, but might have a significant effect on the system.

Secondly, there is only one dimension taken into account in the description of the system, this is the spatial coordinate $l$. If the radius of the tube becomes big relative to the length of the tube, this simplification could lead to different results in the system, since there could be flows in the direction of the other spatial coordinates $r$ and $\theta$ which could be of importance.
For example if the radius of the horizontal tubes is large enough, velocities in the direction of spatial coordinates $r$ and $\theta$ can exist by natural convection, which most likely will influence the heat transfer from the fluid to the wall of the tube. This causes different results of the temperature and since this is connected also a different result of the velocity in the direction of the spatial coordinate $l$.

Thirdly some parameters were taken to be constant in the system, but are dependent on the temperature in the system, like the specific heat capacity, the thermal expansion coefficient and the thermal conductivity. When these parameters are taken as temperature dependent, this could off course affect the system. Since the parameters than will be different at different locations of the tube, which affects the heat transfer in these different parts. This will most likely cause the temperature profile to be different from the temperature profile obtained in this thesis.

# 6 Conclusion

The in section 1 stated goals of this thesis are now repeated and answered.

– *What influence do the measures of the setup have on the natural convection within this system?*

The measurements of the following four properties all influence the behaviour of the natural convection in this system: the thicknesses of the cooling and heating walls, the radius of the tube and the place in the system where the wall changes thickness.

Firstly, a thinner cooling wall and a thicker heating wall both causes a higher fluid velocity. The reason for this higher velocity is that with a smaller cooling wall and/or a thicker heating wall the temperature differences of the fluid become larger inside the tube resulting in a larger density difference, which causes a higher velocity.
For safety reasons it is important to note that both the thickness of the heating and the cooling wall causes a rise of the temperature when these are thicker.

Secondly, when the radius of the tube becomes bigger the velocity drops quickly. Under variation of the radius the highest temperature inside the loop does not change very much.

Lastly, the length of the heating and cooling region is changed, so the place where the wall changes from a thick wall to a thin wall. This variation results in different velocities. The values of these velocities are still desirable. The velocity is highest when the wall changes at approximately $l = 0.4L$ in the loop, with $L$ the length of the tube and $l$ a spatial coordinate within the tube.

Altogether, this system is very dependent on the thicknesses of the cooling and heating walls and the radius of the tube. However, the place in the system where the wall changes thickness does not influence the steady state velocity and temperatures that much.

– *What will the production be which can be achieved by this system?*

The achievable order of magnitude of the production will be around $10^{-8}$ mg molybdenum$^{99}$ per week. This is very low in comparison to systems treated by others, for example, by Haffmans [19]. The production of the system is again dependent on the measurements of the setup since this is linearly dependent on the volume of the fluid inside this system. The main restriction for the production is the maximum of these measurements. However, the most important reason for the low production is the relatively small neutron cross section for neutron capture .

– *What are the differences and similarities between the numerical and analytical results of this system?*

The time dependent numerical method and the time independent numerical methods give effectively the same steady state solution. For the temperature profile, the analytical method gives a steady state result which is of the same form, but the values are slightly shifted in comparison to the results obtained with the numerical methods. This is due to the fact that simplifications were made to solve the model analytically. Despite these simplifications, the overestimation of the temperature and velocity are relatively small. So the analytical method gives promising results.

Thus it is now known that the system is stable and has a steady state solution, this solution is quite dependent on the measurements in the setup. This solution can be determined with both the Runga Kutta method and the Newton Raphson method. The analytical method gives a good estimation of the system, but the values are a bit shifted from the actual values.

However, currently the main constraint for this setup is the relatively low production. This can not easily be raised, because the system has to be placed inside the DLDR tube in the HOR and the most important restriction is its size.

## 6.1   Recommendations

Firstly, it is recommended for further research to look into if there are ways to increase the production of molybdenum[99]. Because the current production is not sufficient yet. Possible ways to increase the production are: using a larger setup or a different reactor with neutrons within a different energy range. In the data from NEA [12] it can be seen that for some higher energies of the neutrons, the neutron cross section for neutron capture will have relatively large peak values. From the same data, it can be seen that for lower energies of the neutrons the neutron cross section for neutron capture will get bigger.

A second recommendation for further research is to investigate the properties of a molybdenum salt solution. These properties affect the model and using the properties of a usable molybdenum salt solution will give more accurate results.

Next also a more complex model could be studied. For example a model that takes the temperature profile in the wall into account and perhaps look into a higher dimensional approach for this system, since in this thesis there is only looked at a 1D approach.

The last recommendation is for the analytical approach. This could be improved by making fewer simplifications in the model, such as increasing the number of regions inside the derivation of the analytical method instead of the four used in this thesis. However, this requires a quite long derivation. This has a high risk of tiny errors, that in turn can have a significant impact on the final results.

# References

[1] World Nuclear Association, *Radioisotopes in Medicine* https://world-nuclear.org/information-library/non-power-nuclear-applications/radioisotopes-research/radioisotopes-in-medicine.aspx

[2] Molybdenum-99 for Medical Imaging. Washington (DC): National Academies Press (US); 2016 Oct 28. Executive Summary. Available from: https://www.ncbi.nlm.nih.gov/books/NBK396162/

[3] Janssen, L.P.B.M & Warmoeskerken, M.M.C.G. (2006). *Transport Phenomena Data Companion* (3th ed.)

[4] van den Akker, H & Mudde, R. (2014). *Fysische transportverschijnselen* (4th ed.)

[5] Rohde, M. (2014). *Nuclear Reactor Thermal Hydraulics* (version 1.1)

[6] Vuik, c. , Vermolen, F.J. , van Gijzen, M.B. & Vuik, M.J. (2018). *Numerical Methods for Ordinary Differential Equations*(2nd ed.)

[7] Xian, L. , Jiang, G. & Yu, H. (2015). *Natural convective heat transfer from a heated slender vertical tube in a cylindrical tank*, NURETH-16

[8] Nalbantis, I., Bellos, V., & Tsakiris, G. (2020). *Erratum for "friction modeling of flood flow simulations" by vasilis bellos, ioannis nalbantis, and george tsakiris.* Journal of Hydraulic Engineering, 146(10).

[9] Carvalho, G. R., Chenlo, F., Moreira, R., & Telis-Romero, J. (2015). *Physicothermal properties of aqueous sodium chloride solutions.* Journal of Food Process Engineering, 38(3), 234–242.

[10] Aleksandrov, A.A. , Dzhuraeva, E.V. & Utenkov, V.F. (2012).*Viscosity of Aqueous Solutions of Sodium Chloride.* Teplofizika Vysokikh Temperatur, 2012, Vol. 50, No. 3, pp. 378–383.

[11] Ahmad, M. (2009). *Medical isotope production can enriched molybdenum-98 replace enriched uranium?* The Nonproliferation Review, 16(2), 285–292.

[12] NEA, Nuclear Energy Agency. *Data bank Janis.* Retrieved July 2, 2021 from https://www.oecd-nea.org/janisweb/book/neutrons/Mo98/MT102/renderer/110

[13] National Center for Biotechnology Information (2021). PubChem Compound Summary for CID 61424, Sodium molybdate. Retrieved June 11, 2021 from https://pubchem.ncbi.nlm.nih.gov/compound/Sodium-molybdate.

[14] National Center for Biotechnology Information (2021). PubChem Compound Summary for CID 104976, Molybdenum-99. Retrieved June 11, 2021 from https://pubchem.ncbi.nlm.nih.gov/compound/Molybdenum-99.

[15] National Center for Biotechnology Information (2021). PubChem Compound Summary for CID 5234, Sodium chloride. Retrieved June 11, 2021 from https://pubchem.ncbi.nlm.nih.gov/compound/Sodium-chloride.

[16] National Center for Biotechnology Information (2021). PubChem Compound Summary for CID 104976, Molybdenum-99. Retrieved June 11, 2021 from https://pubchem.ncbi.nlm.nih.gov/compound/Molybdenum-99.

[17] Aleksandrov, A.A. , Dzhuraeva, E.V. & Utenkov, V.F. *Viscosity of Aqueous Solutions of Sodium Chloride* 2012, published in Teplofizika Vysokikh Temperatur, 2012, Vol. 50, No. 3, pp. 378–383.

[18] Dresen, L.R. *THE MPML: $^{99}$Molybdenum Producing Mini Loop, driven by natural circulation*, Delft University of Technology, 2019.

[19] Haffmans, L.T.B. *A feasibility and safety evaluation of the 99Molybdenum Producing Mini Loop*, Delft University of Technology, 2021.

[20] Elgin, K. *A study of the feasibility of $^{99}$Mo production inside the TU Delft Hoger Onderwijs Reactor*, Delft University of Technology, 2014.

[21] Huisman, M.V. *MEDICAL ISOTOPE PRODUCTION REACTOR*, Delft University of Technology, 2013.

[22] Huisman, J.A.R. *Heat Transfer of the Mo-99 Research Loop*, Delft University of Technology, 2016.

[23] Pothoven, C.C. *Recirculation of the Mo-99 research loop*, Delft University of Technology, 2016.

[24] Pendse, S. *COOLING SYSTEM DESIGN FOR $^{99}MO$ RESEARCH LOOP* , Delft University of Technology, 2018.

# Appendices

## A  Python Code

Like already mentioned in this thesis, a python code with several scripts was made. One script was made to define the parameters and geometry, two scripts were made for the Runga Kutta method, one script was made for the Newton Raphson method and finally four scripts were made to obtain most of the plots shown in the results.

This python code can be found at GitHub, through the following link or through the QR-code in figure 33,
`https://github.com/rr1229/GithubBEP`



Figure 33: *QR-code to GitHub, where the python code used in this thesis is saved.*

# B Derivation of temperature equations

The energy balance is described in the equation (.1) [5],

$$\rho C_p \frac{DT}{Dt} = q''' - \nabla q'' + T\frac{DP}{Dt} + \bar{\bar{\tau}} : \nabla \boldsymbol{v}. \tag{.1}$$

Fourier's law is used in this derivation and the following approximations are used. The influence of the pressure changes on the energy is assumed to be negligible, so $\frac{DP}{Dt} = 0$. Also this model approximate the influence on the energy by friction to be zero, so $\bar{\bar{\tau}} : \nabla v = 0$. For this system, it will be useful to work in cylindrical coordinates, since the system is a cylindrical shaped pipe. Thus equation (.2) will be used for this system,

$$\rho C_p \left( \frac{\partial T}{\partial t} + v_r \frac{\partial T}{\partial r} + \frac{v_\theta}{r}\frac{\partial T}{\partial \theta} + v_l \frac{\partial T}{\partial l} \right) = q''' - \left( \frac{1}{r}\frac{\partial (rq_r'')}{\partial r} + \frac{1}{r}\frac{\partial q_\theta''}{\partial \theta} + \frac{\partial q_l''}{\partial l} \right). \tag{.2}$$

Then Fourier's Law, $q'' = -k\nabla T$, can be used from which equation (**??**) is obtained,

$$\rho C_p \left( \frac{\partial T}{\partial t} + v_r \frac{\partial T}{\partial r} + \frac{v_\theta}{r}\frac{\partial T}{\partial \theta} + v_l \frac{\partial T}{\partial l} \right) = q''' + k\left( \frac{1}{r}\frac{\partial}{\partial r}\left( r\frac{\partial T}{\partial r} \right) + \frac{1}{r^2}\frac{\partial^2 T}{\partial \theta^2} + \frac{\partial^2 T}{\partial l^2} \right). \tag{.3}$$

In this system, the temperature is investigated in two regions: the temperature of the wall and the temperature of the fluid inside the tube.

For the fluid inside the tube, the velocity in the direction $\theta$ and $r$ is approximated to be zero. The velocity $v$ will be taken equal to the velocity $v_l$ since this is the only velocity in the system. This model also neglects the heat production caused by the neutron capture inside the fluid, from this equation (.4) follows,

$$\rho_0 C_p \left( \frac{\partial T}{\partial t} + v \frac{\partial T}{\partial l} \right) = k\left( \frac{1}{r}\frac{\partial}{\partial r}\left( r\frac{\partial T}{\partial r} \right) + \frac{1}{r^2}\frac{\partial^2 T}{\partial \theta^2} + \frac{\partial^2 T}{\partial l^2} \right), \tag{.4}$$

with $\rho_0$ the fixed density of the fluid, $T$ the temperature of the fluid, $v$ the velocity of the fluid within the tube and $C_p$ the specific heat of the fluid.

When looked at wall region, heat production due to the gamma radiation is present. Also, the velocity in all directions can be taken to be zero, since the material is in solid state. So for this region equation (.5) is valid,

$$\rho_{wall} C_{p_{wall}} \frac{\partial T_B}{\partial t} = q''' + k\left( \frac{1}{r}\frac{\partial}{\partial r}\left( r\frac{\partial T_B}{\partial r} \right) + \frac{1}{r^2}\frac{\partial^2 T_B}{\partial \theta^2} + \frac{\partial^2 T_B}{\partial l^2} \right), \tag{.5}$$

with $\rho_{wall}$ the density of the wall, $T_B$ is the temperature of the wall and $C_{p_{wall}}$ the specific heat of the wall.

## B.1 Analytical method, derivation of temperature equations

To derive an ordinary differential equation which is only dependent on the temperature $T$, the spatial coordinate $l$ and known parameters, an expression has to be obtained for the temperature of the wall. To calculate the temperature of the wall at each location, first a look have to be taken at the intersection of the tube. At every intersection within the tube, the balance described in equation (.6) is valid,

$$q'''\pi((R+\delta R(l))^2 - R^2) = -\frac{\partial \phi_{AB}}{\partial l} + \frac{\partial \phi_{BC}(l)}{\partial l}, \tag{.6}$$

which makes sure that the energy generated in the wall is equal to the energy leaving the wall, which is the case for a system in steady state. When equation (.6) is rewritten the equation described in equation (.7) is obtained,

$$u\rho_{wall}\pi((R+\delta R(l))^2 - R^2) = -h_{AB}2\pi R(T(l) - T_B(l)) + h_{BC}2\pi(R+\delta R(l))(T_B(l) - T_C). \tag{.7}$$

This equation (.7) can again be rewritten into an equation for the temperature of the wall, which has to be determined, visible in equation (.8),

$$T_B(l) = \frac{h_{AB}2R(T(l)) + h_{BC}2(R+\delta R(l))(T_C) + u\rho_{wall}((R+\delta R(l))^2 - R^2)}{(h_{AB}2R + h_{BC}2(R+\delta R(l)))}. \tag{.8}$$

Then equation (.8) and equation (4.16) can be combined. Thus now an expression is obtained for the derivative of the temperature in the fluid with respect to the place in the tube dependent on the temperature of the fluid at a certain location and the velocity of the fluid. The rest of the parameters are all known. This expression is stated in equation (.9),

$$\pi R^2 \rho_0 C_p \left( v\frac{\partial T}{\partial l} \right) = u\rho_{wall}\pi((R+\delta R(l))^2 - R^2) - h_{BC}2\pi(R+\delta R(l))\left( T_B(l) - T_C \right),$$
$$\text{with } T_B(l) = \frac{h_{AB}2R(T(l)) + h_{BC}2(R+\delta R(l))(T_C) + u\rho_{wall}((R+\delta R(l))^2 - R^2)}{(h_{AB}2R + h_{BC}2(R+\delta R(l)))}. \tag{.9}$$

When the expression of the temperature of the wall is filled into the equation of the derivative of the temperature in the fluid with respect to the place in the tube, equation (.10) is obtained,

$$\pi R^2 \rho_0 C_p \left( v\frac{\partial T}{\partial l} \right) = \frac{h_{AB}2u\rho_{wall}\pi R\,\delta R(l)(2R+\delta R(l)) + h_{BC}2u\rho_{wall}\pi\delta R(l)(2R+\delta R(l))(R+\delta R(l))}{h_{AB}2R + h_{BC}2(R+\delta R(l))}$$
$$-\left(\frac{h_{BC}4\pi h_{AB}(R+\delta R(l))RT(l) + h_{BC}^2 4\pi(R+\delta R(l))^2 T_C + h_{BC}2\pi u\rho_{wall}\delta R(l)((2R+\delta R(l))(R+\delta R(l))}{(h_{AB}2R + h_{BC}2(R+\delta R(l)))}\right.$$
$$\left.\frac{-(h_{AB}h_{BC}4\pi R(R+\delta R(l))T_C + h_{BC}^2 4\pi(R+\delta R(l))^2 T_C)}{h_{AB}2R + h_{BC}2(R+\delta R(l))}\right). \tag{.10}$$

When equation (.10) is simplified by the terms which fall out equation (.11) is left,

$$\left( v\frac{\partial T}{\partial l} \right) = \frac{h_{AB}u\rho_{wall}R\,\delta R(l)(2R+\delta R(l)) - h_{BC}h_{AB}2(R+\delta R(l))R\left( T(l) - T_c \right)}{R^2 \rho_0 C_p(h_{AB}R + h_{BC}(R+\delta R(l)))}. \tag{.11}$$

To determine an expression for the temperature it is used that the velocity is constant in this system. Thus the differential equation in equation (.12) has to be solved,

$$\frac{\partial T}{\partial l} = \frac{h_{AB}((2R+\delta R(l))u\rho_{wall}\delta R(l) + 2(R+\delta R(l))h_{BC}T_C) - h_{BC}h_{AB}2(R+\delta R(l))T(l)}{vR\rho_0 C_p(h_{AB}R + h_{BC}(R+\delta R(l)))}. \tag{.12}$$

To give a more clear view of equation (.12) all the known parameters will be defined through the constants $A(l)$ and $B(l)$ shown in equation (.13),

$$B(l) = \frac{h_{AB}\,\delta R(l)\,(2R+\delta R(l))\,u\,\rho_{wall} + 2h_{AB}\,h_{BC}\,(R+\delta R(l))\,T_C)}{v\,R\,\rho_0\,C_p\,(h_{AB}R + h_{BC}(R+\delta R(l)))},$$
$$A(l) = \frac{-h_{BC}\,h_{AB}\,2(R+\delta R(l))}{v\,R\,\rho_0\,C_p\,(h_{AB}R + h_{BC}(R+\delta R(l)))}. \tag{.13}$$

The thickness of the tube is dependent on the location in this case. In this thesis, there will be assumed that there are 4 different regions with a constant thickness of the tube: $[0(=L_0), L_1], [L_1, L_2], [L_2, L_3]$ and $[L_3, L_4]$. When applying this to the constants $A(l)$ and $B(l)$ the expression (.14) is valid,

$$B(l) = \mathbb{1}_{[0,L_1]}(l)B_1 + \mathbb{1}_{[L_1,L_2]}(l)B_2 + \mathbb{1}_{[L_2,L_3]}(l)B_3 + \mathbb{1}_{[L_3,L_4]}(l)B_4,$$
$$A(l) = \mathbb{1}_{[0,L_1]}(l)A_1 + \mathbb{1}_{[L_1,L_2]}(l)A_2 + \mathbb{1}_{[L_2,L_3]}(l)A_3 + \mathbb{1}_{[L_3,L_4]}(l)A_4, \tag{.14}$$

with $\mathbb{1}$ the indicator function, so this is of the form stated in equation (.15),

$$\mathbb{1}_{[A,B]}(l) = \begin{cases} 1 & l \in [A, B], \\ 0 & l \notin [A, B]. \end{cases} \tag{.15}$$

The constant $A_n$ is defined as the following: $A_1$, $A_2$, $A_3$ and $A_4$ which are the values of $A(l)$ with the location $l$ in respectively $[0, L_1], [L_1, L_2], [L_2, L_3]$ and $[L_3, L_4]$. The same system is used for the parameters $B_n$ with the function $B(l)$.

So differential equation (.16) is obtained which has to be solved,

$$\frac{\partial T}{\partial l} = \sum_{n=1}^{4} (B_n + A_n T(l))\mathbb{1}_{[L_{n-1}, L_n]}. \tag{.16}$$

To solve this, there has to be looked separately at the different regions and later these must be connected with the boundary conditions.

First a look is taken at the system in the region $[L_{n-1}, L_n]$ with $1 \leq n \leq 4$, so $l \in [L_{n-1}, L_n]$. The equation which has to be solved has become equation (.17),

$$\frac{\partial T_n}{\partial l} = B_n + A_n T_n(l)). \tag{.17}$$

Then the expression $\hat{T}(l) = T_n(l) + \frac{Bn}{An}$ is taken to solve this differential equation. From this equation (.18) is obtained to be solved,

$$\frac{\partial \hat{T}(l)}{\partial l} = \frac{\partial(\hat{T}(l) - \frac{Bn}{An})}{\partial l} = B_n + A_n\left(\hat{T}(l) - \frac{Bn}{An}\right) = A_n\hat{T}(l). \tag{.18}$$

This differential equation is easily solved. Solution (.19) is than obtained,

$$\hat{T}(l) = \alpha_n e^{A_n l}, \tag{.19}$$

with $\alpha_n$ a constant. Going back to the original temperature, the solution described in equation (.20) is obtained for the region $[L_{n-1}, L_n]$,

$$T_n(l) = -\frac{B_n}{A_n} + \alpha_n e^{A_n l}. \tag{.20}$$

To know the expression for the constant $\alpha_n$ the boundary conditions described in equation (.21) are used,

$$\begin{aligned} T_1(L_1) &= T_2(L_1), \\ T_2(L_2) &= T_3(L_2), \\ T_3(L_3) &= T_4(L_3), \\ T_4(L_4) &= T_1(0). \end{aligned} \tag{.21}$$

When this boundary conditions are applied an equation is obtained for each boundary condition, which are stated in equation (.22)

$$\begin{aligned} -\frac{B_1}{A_1} + \alpha_1 e^{A_1 L_1} &= -\frac{B_2}{A_2} + \alpha_2 e^{A_2 L_1}, \\ -\frac{B_2}{A_2} + \alpha_2 e^{A_2 L_2} &= -\frac{B_3}{A_3} + \alpha_3 e^{A_3 L_2}, \\ -\frac{B_3}{A_3} + \alpha_3 e^{A_3 L_3} &= -\frac{B_4}{A_4} + \alpha_4 e^{A_4 L_3}, \\ -\frac{B_4}{A_4} + \alpha_4 e^{A_4 L_4} &= -\frac{B_1}{A_1} + \alpha_1 e^{A_1 0} = -\frac{B_1}{A_1} + \alpha_1. \end{aligned} \tag{.22}$$

When the expressions in equation (.22) are rewritten, the equations for the constants $\alpha_n$ are obtained as shown in equation (.23),

$$
\begin{aligned}
\alpha_1 &= \left( -\frac{B_2}{A_2} + \alpha_2 e^{A_2 L_1} + \frac{B_1}{A_1} \right) e^{-A_1 L_1}, \\
\alpha_2 &= \left( -\frac{B_3}{A_3} + \alpha_3 e^{A_3 L_2} + \frac{B_2}{A_2} \right) e^{-A_2 L_2}, \\
\alpha_3 &= \left( -\frac{B_4}{A_4} + \alpha_4 e^{A_4 L_3} + \frac{B_3}{A_3} \right) e^{-A_3 L_3}, \\
\alpha_4 &= \left( -\frac{B_1}{A_1} + \alpha_1 + \frac{B_4}{A_4} \right) e^{-A_4 L_4}.
\end{aligned}
\tag{.23}
$$

As can be seen in equation (.23) the constants are dependent on each other, when these expressions are filled in and worked out, an expression for $\alpha_1$ is obtained, which is shown in equation (.24),

$$
\begin{aligned}
\alpha_1 =& (1 - e^{-A_4 L_4 + A_4 L_3 - A_3 L_3 + A_3 L_2 - A_2 L_2 + A_2 L_1 - A_1 L_1})^{-1} \\
&\cdot \Bigg( -\frac{B_2}{A_2} e^{-A_1 L_1} - \frac{B_3}{A_3} e^{-A_2 L_2 + A_2 L_1 - A_1 L_1} \\
&- \frac{B_4}{A_4} e^{-A_3 L_3 + A_3 L_2 - A_2 L_2 + A_2 L_1 - A_1 L_1} \\
&- \frac{B_1}{A_1} e^{-A_4 L_4 + A_4 L_3 - A_3 L_3 + A_3 L_2 - A_2 L_2 + A_2 L_1 - A_1 L_1} \\
&+ \frac{B_4}{A_4} e^{-A_4 L_4 + A_4 L_3 - A_3 L_3 + A_3 L_2 - A_2 L_2 + A_2 L_1 - A_1 L_1} \\
&+ \frac{B_3}{A_3} e^{-A_3 L_3 + A_3 L_2 - A_2 L_2 + A_2 L_1 - A_1 L_1} \\
&+ \frac{B_2}{A_2} e^{-A_2 L_2 + A_2 L_1 - A_1 L_1} + \frac{B_1}{A_1} e^{-A_1 L_1} \Bigg).
\end{aligned}
\tag{.24}
$$

When equation (.24) is reformulated equation (.25) obtained,

$$
\begin{aligned}
\alpha_1 =& (1 - e^{-A_4 L_4 + A_4 L_3 - A_3 L_3 + A_3 L_2 - A_2 L_2 + A_2 L_1 - A_1 L_1})^{-1} \\
&\cdot \Bigg( \left( \frac{B_1}{A_1} - \frac{B_2}{A_2} \right) e^{-A_1 L_1} \\
&+ \left( \frac{B_2}{A_2} - \frac{B_3}{A_3} \right) e^{-A_2 L_2 + A_2 L_1 - A_1 L_1} \\
&+ \left( \frac{B_3}{A_3} - \frac{B_4}{A_4} \right) e^{-A_3 L_3 + A_3 L_2 - A_2 L_2 + A_2 L_1 - A_1 L_1} \\
&+ \left( \frac{B_4}{A_4} - \frac{B_1}{A_1} \right) e^{-A_4 L_4 + A_4 L_3 - A_3 L_3 + A_3 L_2 - A_2 L_2 + A_2 L_1 - A_1 L_1} \Bigg).
\end{aligned}
\tag{.25}
$$

Thus the solution to the differential equation of the temperature with respect to the spatial coordinate $l$ is shown in equation (.26),

$$
\begin{cases}
T(l) = \sum_{n=1}^{4} \left( -\frac{B_n}{A_n} + \alpha_n e^{A_n l} \right) \mathbb{1}_{[L_{n-1}, L_n]}, \\[2ex]
\text{with} \quad B_n = \frac{h_{AB_n}\, \delta R_n\, (2R + \delta R_n)\, u\, \rho_{wall} + 2 h_{AB_n}\, h_{BC_n}\, (R + \delta R_n)\, T_C)}{v\, R\, \rho_0\, C_p\, (h_{AB_n}\, R + h_{BC_n}\, (R + \delta R_n))}, \\[2ex]
A_n = \frac{-h_{BC_n}\, h_{AB_n}\, 2(R + \delta R_n)}{v\, R\, \rho_0\, C_p\, (h_{AB_n}\, R + h_{BC_n}\, (R + \delta R_n))}, \\[2ex]
\alpha_1 = \left(1 - e^{-A_4 L_4 + A_4 L_3 - A_3 L_3 + A_3 L_2 - A_2 L_2 + A_2 L_1 - A_1 L_1}\right)^{-1} \\[1ex]
\qquad \cdot \Bigg( \quad \left( \frac{B_1}{A_1} - \frac{B_2}{A_2} \right) e^{-A_1 L_1} \\[1ex]
\qquad\quad + \left( \frac{B_2}{A_2} - \frac{B_3}{A_3} \right) e^{-A_2 L_2 + A_2 L_1 - A_1 L_1} \\[1ex]
\qquad\quad + \left( \frac{B_3}{A_3} - \frac{B_4}{A_4} \right) e^{-A_3 L_3 + A_3 L_2 - A_2 L_2 + A_2 L_1 - A_1 L_1} \\[1ex]
\qquad\quad + \left( \frac{B_4}{A_4} - \frac{B_1}{A_1} \right) e^{-A_4 L_4 + A_4 L_3 - A_3 L_3 + A_3 L_2 - A_2 L_2 + A_2 L_1 - A_1 L_1} \Bigg), \\[2ex]
\alpha_4 = \left( -\frac{B_1}{A_1} + \alpha_1 + \frac{B_4}{A_4} \right) e^{-A_4 L_4}, \\[2ex]
\alpha_3 = \left( -\frac{B_4}{A_4} + \alpha_4 e^{A_4 L_3} + \frac{B_3}{A_3} \right) e^{-A_3 L_3}, \\[2ex]
\text{and} \quad \alpha_2 = \left( -\frac{B_3}{A_3} + \alpha_3 e^{A_3 L_2} + \frac{B_2}{A_2} \right) e^{-A_2 L_2}.
\end{cases}
\tag{.26}
$$

## C Velocity

The Navier Stokes equation for Newtonian fluids with constant density is stated in equation (.27) [3],

$$\rho\frac{\partial \boldsymbol{v}}{dt} + \rho\boldsymbol{v}\cdot\nabla\boldsymbol{v} = \nabla P + \mu\nabla^2\boldsymbol{v} + \rho\boldsymbol{g}. \tag{.27}$$

An more extensive form of equation (.27) are the equations shown in equation (.28),

$$\rho\left[\frac{\partial v_x}{dt} + v_x\frac{\partial v_x}{dx} + v_y\frac{\partial v_x}{dy} + v_z\frac{\partial v_x}{dz}\right] = -\frac{\partial P}{dx} + \mu\left(\frac{\partial^2 v_x}{\partial x^2} + \frac{\partial^2 v_x}{\partial y^2} + \frac{\partial^2 v_x}{\partial z^2}\right) + \rho g_x,$$

$$\rho\left[\frac{\partial v_y}{dt} + v_x\frac{\partial v_y}{dx} + v_y\frac{\partial v_y}{dy} + v_z\frac{\partial v_y}{dz}\right] = -\frac{\partial P}{dy} + \mu\left(\frac{\partial^2 v_y}{\partial x^2} + \frac{\partial^2 v_y}{\partial y^2} + \frac{\partial^2 v_y}{\partial z^2}\right) + \rho g_y, \tag{.28}$$

$$\rho\left[\frac{\partial v_z}{dt} + v_x\frac{\partial v_z}{dx} + v_y\frac{\partial v_z}{dy} + v_z\frac{\partial v_z}{dz}\right] = -\frac{\partial P}{dz} + \mu\left(\frac{\partial^2 v_z}{\partial x^2} + \frac{\partial^2 v_z}{\partial y^2} + \frac{\partial^2 v_z}{\partial z^2}\right) + \rho g_z,$$

with $\mu$ the dynamic viscosity. For this system cylindrical coordinates are useful, equation (.28) stated in cylindrical coordinates is shown in equation (.29),

$$\rho\left[\frac{\partial v_r}{\partial t} + v_r\frac{\partial(rv_r)}{\partial r} + v_\theta\frac{\partial v_r}{d\theta}\frac{1}{r} - \frac{v_\theta^2}{r} + v_l\frac{\partial v_r}{\partial l}\right] = -\frac{\partial P}{\partial r} + \mu\left(\frac{\partial}{\partial r}\left(\frac{\partial(rv_r)}{\partial r}\frac{1}{r}\right) + \frac{\partial^2 v_r}{\partial\theta^2}\frac{1}{r^2} - \frac{2}{r^2}\frac{\partial v_\theta}{\partial\theta} + \frac{\partial^2 v_r}{\partial l^2}\right) + \rho g_r,$$

$$\rho\left[\frac{\partial v_\theta}{\partial t} + v_r\frac{\partial v_\theta}{\partial r} + v_\theta\frac{\partial v_\theta}{d\theta}\frac{1}{r} + \frac{v_r v_\theta}{r} + v_l\frac{\partial v_\theta}{\partial l}\right] = -\frac{\partial P}{d\theta}\frac{1}{r} + \mu\left(\frac{\partial}{\partial r}\left(\frac{\partial(rv_\theta)}{\partial r}\frac{1}{r}\right) + \frac{\partial^2 v_\theta}{\partial\theta^2}\frac{1}{r^2} + \frac{2}{r^2}\frac{\partial v_r}{\partial\theta} + \frac{\partial^2 v_\theta}{\partial l^2}\right) + \rho g_\theta,$$

$$\rho\left[\frac{\partial v_l}{\partial t} + v_r\frac{\partial v_l}{\partial r} + v_\theta\frac{\partial v_l}{d\theta}\frac{1}{r} + v_l\frac{\partial v_l}{dl}\right] = -\frac{\partial P}{dl} + \mu\left(\frac{1}{r}\frac{\partial}{\partial r}\left(\frac{\partial rv_l}{\partial r}r\right) + \frac{\partial^2 v_l}{\partial\theta^2}\frac{1}{r^2} + \frac{\partial^2 v_l}{\partial l^2}\right) + \rho g_l. \tag{.29}$$

To look at a 1D system it will be assumed that this system is independent of $r$ & $\theta$ and $v_r = v_\theta = 0$. With this assumptions equation (.30) is obtained,

$$\rho\frac{\partial v_l}{\partial t} + \rho v_l\frac{\partial v_l}{\partial l} = -\frac{\partial P}{\partial l} + \mu\frac{\partial^2 v_l}{\partial l^2} + \rho g\sin(\phi). \tag{.30}$$

In this system the assumption is made that $v_l$ is constant over $l$. From this the expression shown in equation (.31) is gotten.

$$\rho\frac{\partial v_l}{\partial t} = -\frac{\partial P}{\partial l} + \rho g\sin(\phi), \tag{.31}$$

with $v_l = v$ , since it is the only velocity present in the system.

### C.1 Analytical velocity

For the analytical method, the equation will be integrated over the length, from which equation (.32) is obtained,

$$0 = \int_0^L -f_D \frac{\rho}{4R} v^2 dl - \int_0^L \kappa(\frac{1}{2}\rho v^2)\delta(l)dl + \int_0^L \rho g \sin(\phi_l)dl. \tag{.32}$$

Since in this system there are four different angles of the gravitational force applied relative to the velocity, this integral can be divided into four different integrals with constant angles, this is shown in equation (.33),

$$v = \left( \frac{g\left( \int_0^{L_1} \rho \sin(\phi_1)dl + \int_{L_1}^{L_2} \rho \sin(\phi_2)dl + \int_{L_2}^{L_3} \rho \sin(\phi_3)dl + \int_{L_3}^{L_4} \rho \sin(\phi_4)dl \right)}{\int_0^L \rho f \frac{1}{4R}dl + \kappa_1 \frac{1}{2}(\rho(L_1) + \rho(L_3)) + \kappa_1 \frac{1}{2}(\rho(L_2) + \rho(0))} \right)^{1/2}. \tag{.33}$$

In this thesis it is assumed that the density is constant except for the changes in the gravitational forces, this gives equation (.34),

$$v = \left( \frac{g\sum_{n=1}^4 \int_{L_{n-1}}^{L_n} \rho \sin(\phi_n)dl}{\rho_0 f \frac{1}{4R}L + \rho_0(\kappa_1 + \kappa_2)} \right)^{1/2}. \tag{.34}$$

Equation (4.23) can again be used in this derivation, from which equation (.35) is obtained for the velocity of the analytical part,

$$v = \left( \frac{g\sum_{n=1}^4 \int_{L_{n-1}}^{L_n} (1 - \beta(T - T_0))\sin(\phi_n)dl}{f \frac{1}{4R}L + (\kappa_1 + \kappa_2)} \right)^{1/2}. \tag{.35}$$

To give a better overview of the equation, again the equation will be split into the function and the constants. In this system, the following is true $\sum_{n=1}^4 \int_{L_{n-1}}^{L_n} (1 + \beta T_0)\sin(\phi_n)dl = 0$, since $\beta$ & $T_0$ are constant, the angles from the pipes are reversed ($sin(\phi_1) = -sin(\phi_3)$, $sin(\phi_2) = -sin(\phi_4)$) and each side of the pipe has an equal length, $\Delta l$ is constant. From this, the expression of the velocity is obtained, which is stated in equation (.36)

$$\begin{cases} v = \left( \sum_{n=1}^4 C_n \int_{L_{n-1}}^{L_n} T(l)dl \right)^{1/2}, \\ C_n = \frac{-g\beta \sin(\phi_n)}{f_D \frac{1}{4R}L + (\kappa_1 + \kappa_2)}. \end{cases} \tag{.36}$$

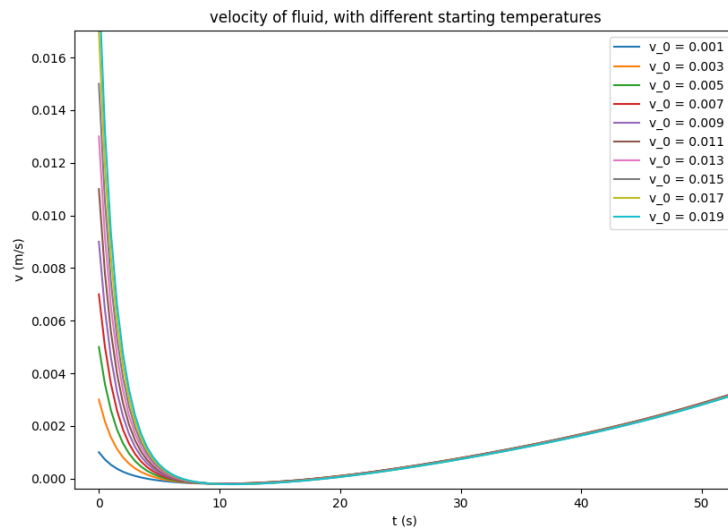# D  Variation of the initial condition

To check if the steady state of this system does not depend on the initial condition, the Runga Kutta method is used with different initial conditions. For the results in this subsection the following values are used, the thickness of the cooling wall $\delta R = 1$mm, the thickness of the heating wall $\delta R = 7$mm, the radius of the tube $R = 3$mm and the point in the tube at which the thickness of the wall is changed is at $l = 0.5L$.

Firstly the initial velocity is varied from $v_0 = 0.001\frac{m}{s}$ till $v_0 = 0.02\frac{m}{s}$ which gives the results shown in figure 34 and figure 35.
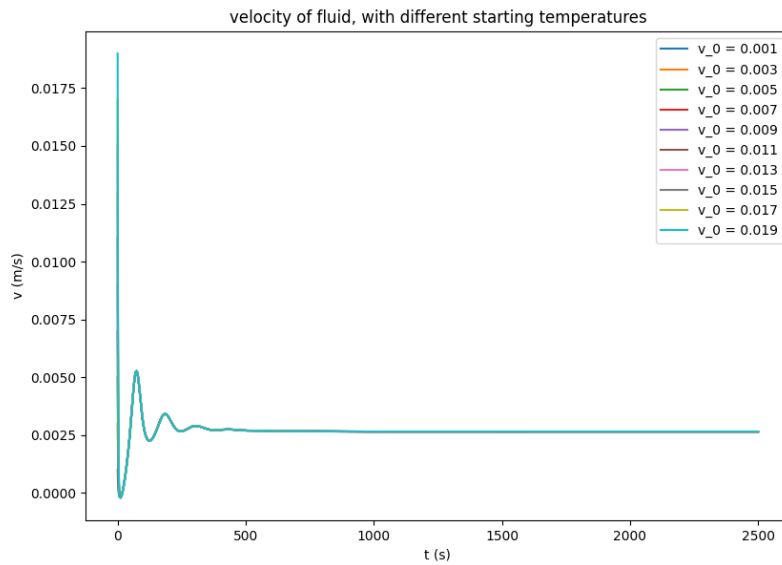


(a) *Velocity of fluid $[\frac{m}{s}]$.*



(b) *Velocity of fluid $[\frac{m}{s}]$, zoomed in.*

Figure 34: *Velocity for variation of the initial velocity from from $v_0 = 0.001\frac{m}{s}$ till $v_0 = 0.02\frac{m}{s}$.*
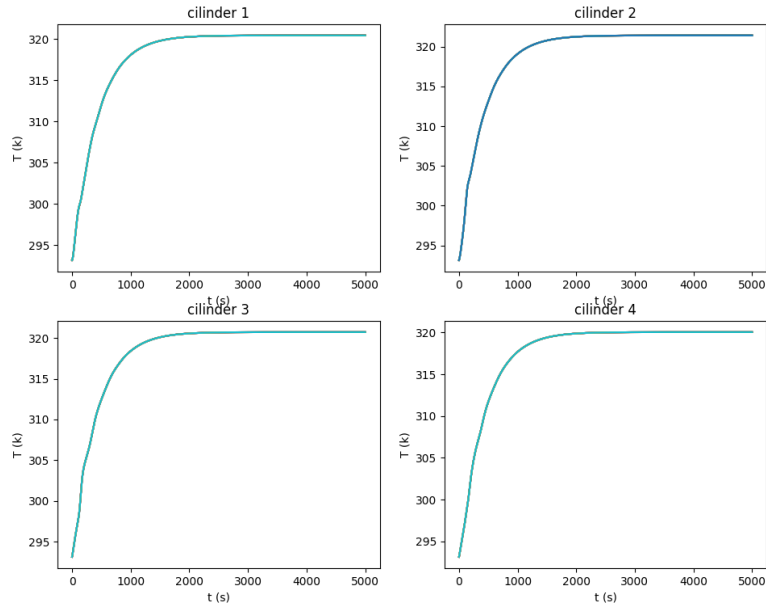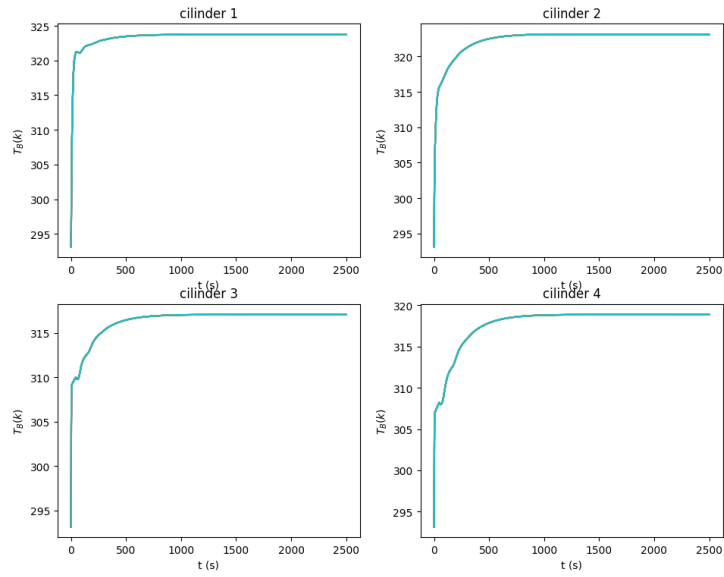
(a) *Temperature in the loop [K].*



(b) *Temperature of the wall [K].*

Figure 35: *Temperature for variation of the initial velocity from from $v_0 = 0.001\frac{m}{s}$ till $v_0 = 0.02\frac{m}{s}$.*

In figure 34a the different velocities are not good visible for different initial velocities, so a zoomed-in plot is added, figure 34b, in which can be seen that the values of the velocity quickly become the same for different initial velocities. Also, the temperatures in the wall and in the fluid stay the same for different initial velocities as can be seen in figure 35b and 35a.

The velocity is also varied for the values of the initial velocity from $v_0 = 0.02\frac{m}{s}$ till $v_0 = 0.2\frac{m}{s}$ and for the the values of the initial velocity from $v_0 = 0.0001\frac{m}{s}$ till $v_0 = 0.001\frac{m}{s}$ which show the same results. The values of the velocities quickly have the same value and the values of the temperature stay the same.

Secondly, the initial conditions of the temperature are varied. The temperature of the wall and of the fluid are first both varied from $T = T_{wall} = 10^oC$ to $T = T_{wall} = 80^oC$. The results of this variation can be seen in figures 36, 37 and 38.
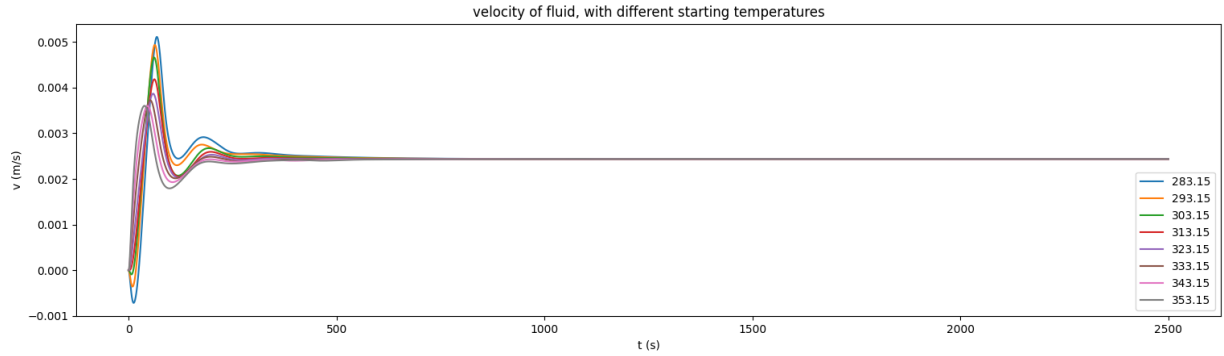


Figure 36: *Velocity of fluid $[\frac{m}{s}]$ for the variation of the initial temperatures from $T = T_{wall} = 10^oC$ to $T = T_{wall} = 80^oC$.*
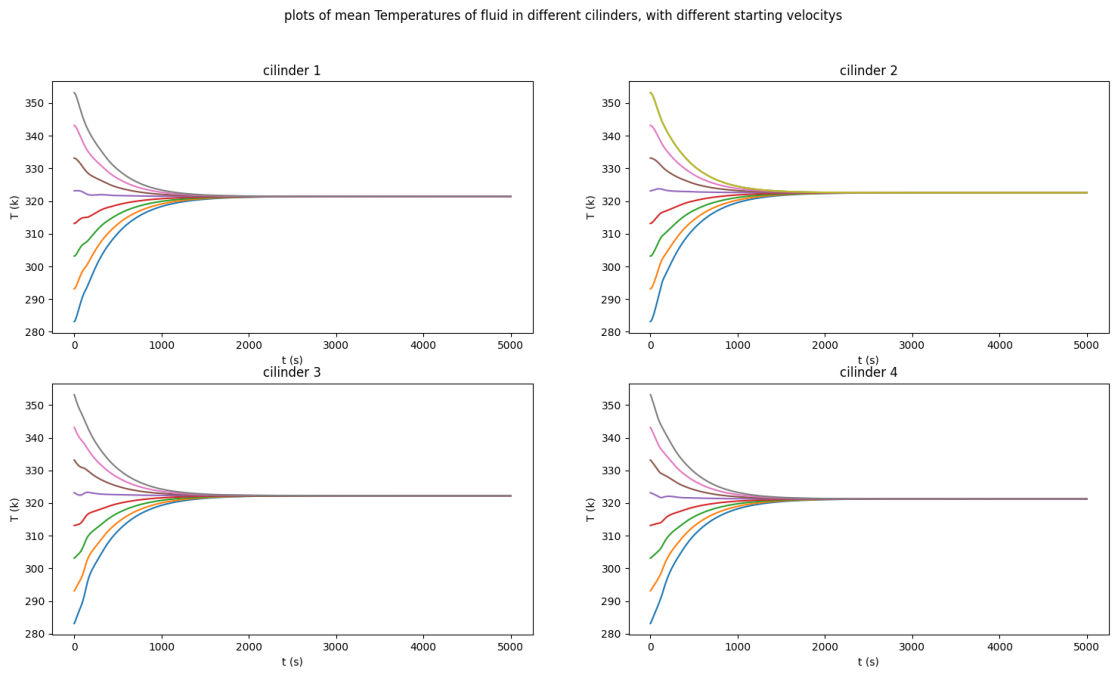


Figure 37: *Temperature of the fluid [K] for the variation of the initial temperatures from $T = T_{wall} = 10^oC$ to $T = T_{wall} = 80^oC$.*
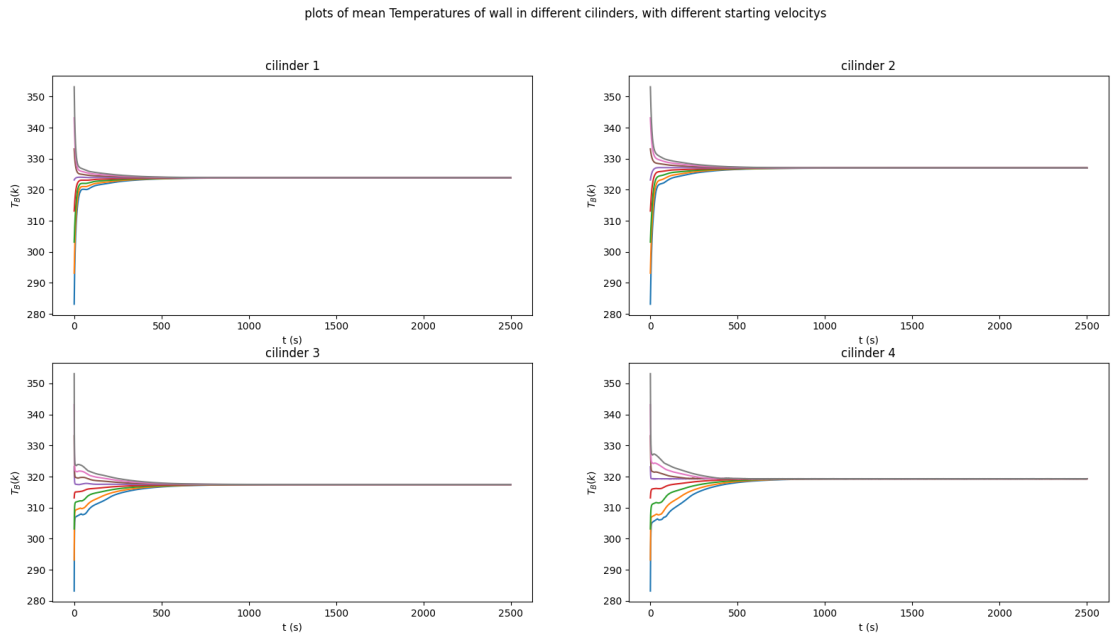
Figure 38: *Temperature of the wall [K] for the variation of the initial temperatures from $T = T_{wall} = 10^oC$ to $T = T_{wall} = 80^oC$.*

In figure 36 can be seen that for this variation, the velocity does not become of the same value as quickly as by the variation of the initial velocity. But over a longer time scale, all the values eventually become the same again. The same can be said for both the temperature of the fluid and the temperature of the wall, which can be seen in figure 37 and figure 38.

Note that the velocity in figure 36 is below zero for some initial temperatures. This is because the initial temperature of the wall is below the temperature of the surrounding water, this causes the system to be heated by the surrounding water at the start. In the part with a thinner wall, this heating is off course faster than in the part with a thicker wall, which causes the temperature in the part of the thinner wall to be temporarily higher than the temperature in the thicker wall. Which in its turn causes the velocity to become negative. When the gamma heating becomes the dominating heating source of the system this will change and the velocity will become positive, which also can be seen in figure 36. When taking the initial temperature of the wall equal to the temperature of the surrounding water it can be seen that this indeed does not occur anymore in figure 39. This figure 39 is together with figures 40a and 40b the result of the variation of only the temperature of the fluid, from $T = 10^oC$ to $T = 60^oC$. In all three these figures, the same conclusions can be made as from the variation of both temperatures.

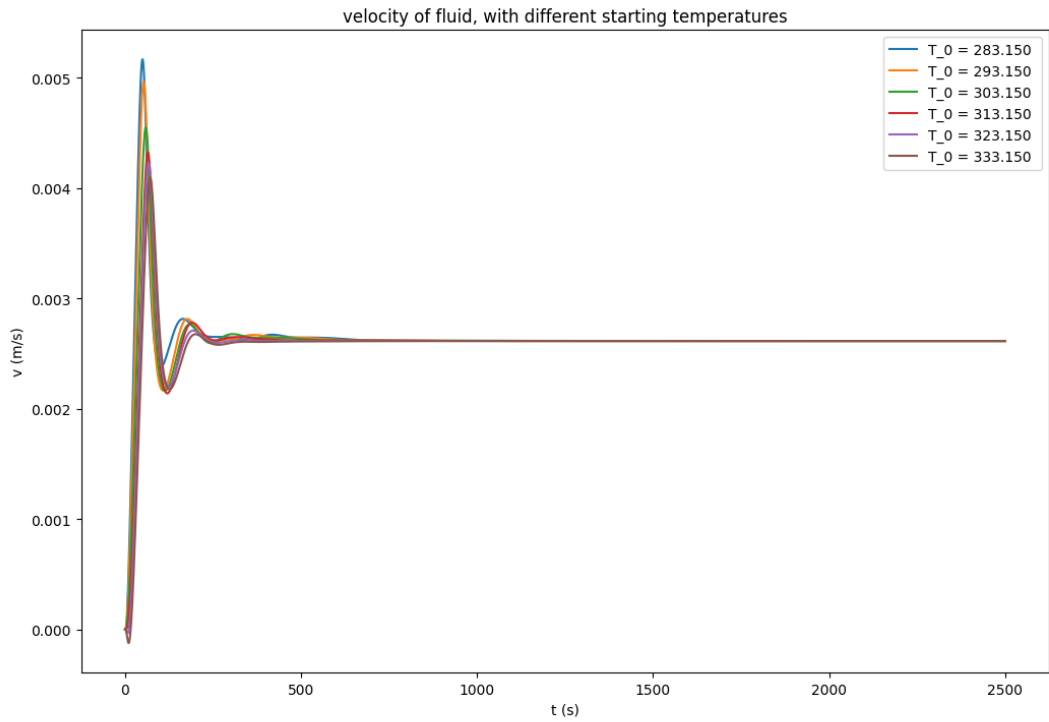Figure 39: *Velocity of fluid $\left[\frac{m}{s}\right]$ with variation of the initial velocity from from $v_0 = 0.001\frac{m}{s}$ till $v_0 = 0.02\frac{m}{s}$.*



(a) *Temperature of the fluid [K].*
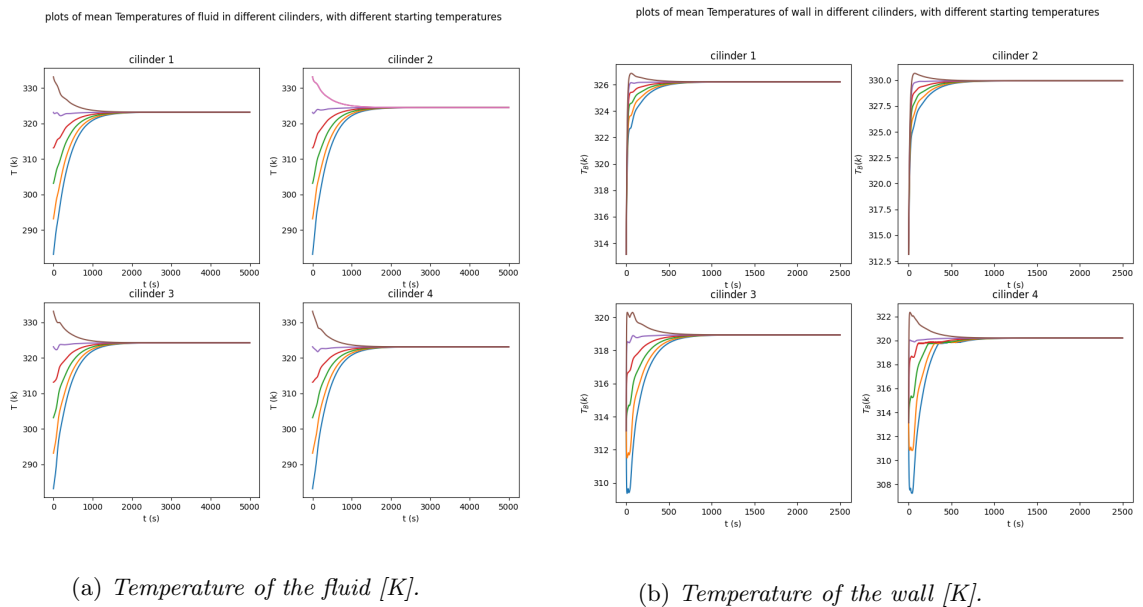
(b) *Temperature of the wall [K].*

Figure 40: *Variation of the initial velocity from from $v_0 = 0.001\frac{m}{s}$ till $v_0 = 0.02\frac{m}{s}$.*

# E  Stability of the system and converges of numerical methods

The stability of the system is dependent on the eigenvalues of the system. When the real part of these eigenvalues are all negative, there can be spoken of a stable system [6]. For the Runga Kutta method, an extra condition is however required. The Runga Kutta method is stable, when the condition, shown in equation (.37), is satisfied [6],

$$\Delta t \leq \frac{-2.8}{\lambda}, \tag{.37}$$

with $\Delta t$ the time step taken in the Runga Kutta method and $\lambda$ the eigenvalues of this system, $f' = \lambda f$. Since it is quite difficult to determine the eigenvalues of such a nonlinear system, the stability will be tested using the Python code. This is tested with the following values, the thickness of the cooling wall $\delta R = 1$mm, the thickness of the heating wall $\delta R = 7$mm, the radius of the tube $R = 3$mm and the point in the tube at which the thickness of the wall is changed is at $l = 0.5L$. The results of this test are shown in figure 41.
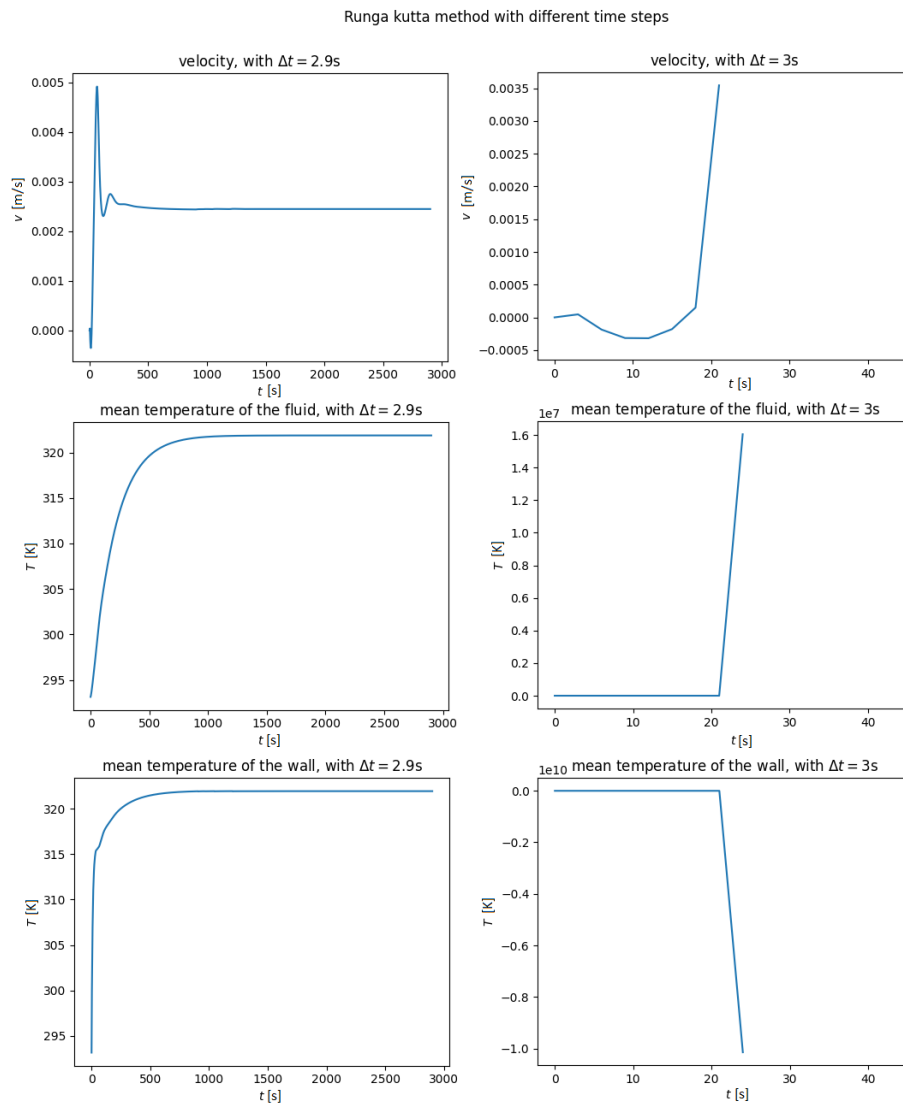


Figure 41: *Results of Runga Kutta method, with from top to bottom respectively the velocity, the mean temperature of the fluid and the mean temperature of the wall. The results obtained with time step $\Delta t = 2.9s$ are shown in the left column and the results obtained with time step $\Delta t = 3s$ are shown in the right column.*

It is found that for these parameters the point at which this condition is not satisfied anymore is between $\Delta t = 2.9$s and $\Delta t = 3$s, this can be seen in figure 41. This means that for times step $\Delta t \leq 2.9$s the Runga Kutta method is stable for the used parameters. To have a stable Runga Kutta method for different systems, in this thesis the time step $\Delta t = 0.5$s is used.

The condition in equation (.37) can only be satisfied if all eigenvalues are negative, since the time steps can not be negative. Because of this and of the fact that the Runga Kutta method is indeed stable for certain values of the time steps, there can be said that the eigenvalues of this system are indeed negative. This means that this system is indeed stable.

The convergence of the methods used for the time independent numerical method, Newton Raphson, and for determining the velocity in the analytical method, an iterative method, are dependent on the initial guess. If this initial guess is close enough to an equilibrium point, the methods will converge. To make sure it will be close enough, the result of the Runga Kutta method is used or an initial guess close to this result.

To make sure there are not multiple equilibrium points where these methods can converge to the initial conditions of the Runga Kutta method where varied, like seen in the previous subsection. Since the Runga Kutta method for different initial conditions goes towards the same equilibrium it is assumed that within the range of values that is probable for this system there is only one equilibrium of the system. This means that for a proper initial guess both the methods will only converge to this equilibrium and for initial guesses which are too far from the equilibrium the methods will not converge to another equilibrium, since this does not exist in the range of values feasible for this model.

# F  Conservation of energy

For this to be a physically feasible system, conservation of energy has to be satisfied. This means that the energy generated inside this system has to be equal to the energy which leaves the system. The only energy generated in this system is in the wall. So the energy which enters and leaves the fluid should be the same. And the energy which leaves the wall in total should be equal to the energy generated in the wall. For both of these remarks, there will be looked at the heat transfer shown in figure 42, which is the heat transport for a system with the following parameters, the thickness of the cooling wall $\delta R = 1$mm, the thickness of the heating wall $\delta R = 7$mm, the radius of the tube $R = 3$mm and the point in the tube at which the thickness of the wall is changed is at $l = 0.5L$.
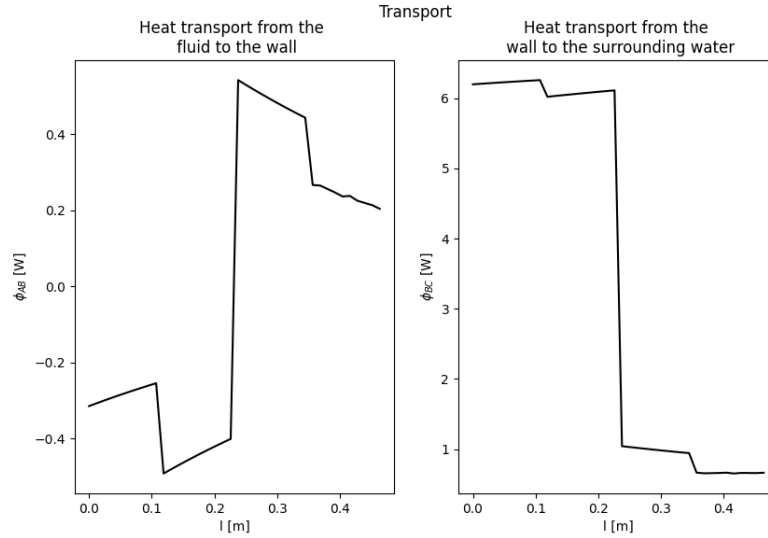


Figure 42: *Heat transport inside the system, with in the left plot the heat transport from the fluid to the wall [W] and in the right plot the heat transport from the wall to the surrounding water [W].*

When the heat transport profiles in figure 42 are numerical integrated over the segments in the region $[0, L]$ with $L$ the length of the tube, the following values are obtained, $\phi_{AB_{total}} = 0.0044$W and $\phi_{BC_{total}} = 140.14$W. This first value is relatively small, the reason this value is not exactly equal to zero is probably because of some accuracy errors and because the system is divided into segments. But the error is acceptably small enough. The second value should be equal to the energy generated inside the wall, which is $P_\gamma = 140.23$W. This has a relatively small error, which is acceptably small enough. So the system seems to, expect from some accuracy errors, satisfy the conservation of energy.